



HAL
open science

Sugarcane radiation use efficiency: varietal differences, temperature dependence, and implications for modeling biomass across environments

Mathias Christina, David Clark, Fabio Ricardo Marin, Rafael Vasconcelos Ribeiro, Julio Victor Saez, Tendai Polite Chibarabada, Murilo dos Santos Vianna, Matthew R. Jones, Santiago Vianna Cuadra, Osvaldo Machado Rodrigues Cabral, et al.

► To cite this version:

Mathias Christina, David Clark, Fabio Ricardo Marin, Rafael Vasconcelos Ribeiro, Julio Victor Saez, et al.. Sugarcane radiation use efficiency: varietal differences, temperature dependence, and implications for modeling biomass across environments. 2025. hal-04942764

HAL Id: hal-04942764

<https://hal.science/hal-04942764v1>

Preprint submitted on 12 Feb 2025

HAL is a multi-disciplinary open access archive for the deposit and dissemination of scientific research documents, whether they are published or not. The documents may come from teaching and research institutions in France or abroad, or from public or private research centers.

L'archive ouverte pluridisciplinaire **HAL**, est destinée au dépôt et à la diffusion de documents scientifiques de niveau recherche, publiés ou non, émanant des établissements d'enseignement et de recherche français ou étrangers, des laboratoires publics ou privés.



Distributed under a Creative Commons Attribution - NonCommercial - NoDerivatives 4.0 International License

1 **Sugarcane radiation use efficiency: varietal differences, temperature dependence, and**
2 **implications for modeling biomass across environments**

3

4 **Authors:** Mathias Christina^{1,2*}, David Clark^{3,4}, Fabio Ricardo Marin⁵, Rafael Vasconcelos
5 Ribeiro⁶, Julio Victor Saez⁷, Tendai Polite Chibarabada^{8,9}, Murilo dos Santos Vianna¹⁰,
6 Matthew R. Jones¹¹, Santiago Vianna Cuadra¹², Osvaldo Machado Rodrigues Cabral¹³, Martin
7 Moises Acreche¹⁴, Henrique Boriolo Dias¹⁵

8

9 ¹ CIRAD, UPR AIDA, F-34398 Montpellier, France

10 ² AIDA, Univ Montpellier, CIRAD, Montpellier, France

11 ³ SASRI, Private Bag X02, Mount Edgecombe, 4300, South Africa

12 ⁴ School of Agricultural, Earth and Environmental Sciences, University of KwaZulu-Natal, Durban
13 4041, South Africa

14 ⁵ University of São Paulo (USP), “Luiz de Queiroz” College of Agriculture (ESALQ), SP 13418-900 PO
15 Box 09 Piracicaba, Brazil

16 ⁶ Laboratory of Crop Physiology, Department of Plant Biology, State University of Campinas, Campinas
17 SP, 13083-862, Brazil

18 ⁷ EEA Famailla, Instituto Nacional de Tecnología Agropecuaria, 4132 Tucumán, Argentina

19 ⁸ Agronomy Department, Zimbabwe Sugar Association Experiment Station, Private Bag 7006, Chiredzi,
20 Zimbabwe

21 ⁹ Centre for Transformative Agricultural and Food Systems, School of Agricultural, Earth and
22 Environmental Sciences, University of KwaZulu-Natal, P. Bag X01, Pietermaritzburg 3209, South
23 Africa

24 ¹⁰ Institute of Bio- and Geosciences (IBG-3), Forschungszentrum Jülich GmbH, 52428, Jülich, Germany

25 ¹¹ Centre for Crop Systems Analysis, Wageningen University and Research, P.O. Box 430, 6700 AK
26 Wageningen, The Netherlands

27 ¹² Empresa Brasileira de Pesquisa Agropecuária, Agricultura Digital, Campinas, SP 13083-886, Brazil

28 ¹³ Empresa Brasileira de Pesquisa Agropecuária, Meio Ambiente, Jaguariúna, SP CEP 13918-110, Brazil

29 ¹⁴ EEA Salta, Instituto Nacional de Tecnología Agropecuaria, CONICET, 4403 Salta, Argentina

30 ¹⁵ Department of Agricultural and Biological Engineering, University of Florida, Gainesville, FL 32611,
31 United States

32

33 * Corresponding author: mathias.christina@cirad.fr; 389 avenue Agropolis, 34980, Montferrier-sur-
34 Lez

35

36

37

38 **Abstract**

39 Sugarcane is a major tropical C4 crop of global economic significance, primarily used for sugar,
40 ethanol, and bioenergy production. As climate change accelerates, with projected increases in
41 global temperatures, understanding the temperature sensitivity of sugarcane's radiation use
42 efficiency (RUE) is crucial for predicting yield under changing environmental conditions. This
43 study aimed to characterize sugarcane RUE response to temperature across various
44 environments and varieties from key producing regions worldwide. Using experimental data
45 from five countries (Brazil, South Africa, United States of America, Zimbabwe, Argentina, and
46 La Réunion) and 40 distinct varieties, our results indicated that maximum RUE (RUE_{MAX})
47 remained consistent across varieties, while apparent RUE (RUE_A) showed significant variation.
48 Based on this dataset, we parameterized different RUE_{MAX} temperature response formalisms
49 used in crop models (APSIM-Sugar, DSSAT-Canegro, MOSICAS, and emergent formalisms).
50 We compared their ability to simulate RUE_A in various regions accurately. Our analysis
51 revealed significant differences in formalism performance, emphasizing the need for accurate
52 parameterization. Additionally, we demonstrated that predictions of biomass production under
53 climate change scenarios are highly sensitive to the formalism parameterization used to
54 represent the RUE-temperature relationship. These findings highlight the critical importance of
55 refining crop models considering temperature response and cardinal temperatures (optimal
56 range: 30–33 °C) to enhance predictions of sugarcane yield under future climate conditions. We
57 discussed several physiological processes that may explain differences in RUE_A among
58 varieties. Incorporating these refined mechanisms into models will support more accurate
59 climate impact assessments and aid breeding programs focused on developing high-yield
60 sugarcane varieties.

61

62 **Keywords:** *Saccharum* spp.; Resource use efficiency; Cultivar; Cardinal temperatures; Climate
63 change; Crop modelling

64

65

66 **Table 1.** Acronyms and definitions.

Acronyms	Units	Definitions
RUE	g DM MJ ⁻¹	Radiation-use efficiency, the rate at which a plant is able to convert intercepted solar radiation into dry biomass.
RUE _A	g DM MJ ⁻¹	Apparent radiation-use efficiency, calculated as total aboveground biomass at final biomass sampling date divided by cumulative intercepted shortwave (global) solar radiation since crop start.
RUE _{MAX}	g DM MJ ⁻¹	The maximum radiation-use efficiency calculated across a sequence of biomass sampling dates in a single cropping season.
RUE _O	g DM MJ ⁻¹	Theoretical maximum radiation-use efficiency under ideal water, temperature, and nutrient conditions.
ADM	t ha ⁻¹	Aboveground dry biomass per area
SRAD	MJ m ⁻² d ⁻¹	Daily shortwave radiation (global solar radiation)
PAR	MJ m ⁻² d ⁻¹	Daily photosynthetically active radiation
<i>f</i> iRAD	MJ MJ ⁻¹	Canopy interception fraction of shortwave (global) solar radiation
<i>i</i> RADc	MJ m ⁻²	Cumulated canopy-intercepted shortwave (global) solar radiation
Anet	μmol m ⁻² s ⁻¹	Instantaneous leaf net photosynthesis
GPP	μmol m ⁻² s ⁻¹	Gross primary productivity

67

68

69 **1. Introduction**

70 Sugarcane (*Saccharum* spp.) is a perennial C4 tropical grass belonging to the Poaceae
71 (Gramineae) family and the genus *Saccharum* (Moore et al., 2013). It is a crop of significant
72 economic importance worldwide, cultivated primarily to produce sugar, ethanol, electricity, and
73 other by-products such as fertilizers, specialty chemicals, paper, and compost (Moore and
74 Botha, 2013). In 2022, around 1.9 billion tons of sugarcane were produced from 26 million ha
75 globally (FAOSTAT database). The demand for sugarcane-derived products is projected to rise
76 in the future, driven by population growth and increasing industrial applications, including
77 biofuels, bioplastics, and other innovative uses (Goldemberg et al., 2014; Leal et al., 2013). To
78 meet this demand, there is a need to avoid extensification and increase yield in existing
79 cultivated areas.

80 Climate change, driven by increases in air temperature in response to increasing
81 concentrations of greenhouse gases (carbon dioxide, methane, and nitrous oxide), is expected
82 to impact future sugarcane production (Dias and Inman-Bamber, 2020; Linnenluecke et al.,
83 2018; Marin et al., 2014; Singels et al., 2021). As temperature change is a primary response to
84 greenhouse gas accumulation in the atmosphere, projected increases in temperature are
85 associated with a relatively low level of uncertainty (Thornton et al., 2014). Global surface
86 mean temperatures have risen by 1.1°C over the last century and are projected to reach +1.5°C
87 in the near term (2030–2035). By 2100, temperatures are expected to increase further, ranging

88 from +1.4°C under a low-emission scenario to +4.4°C under a high-emission scenario (IPCC,
89 2023). Tropical regions, where sugarcane is predominantly grown, are expected to experience
90 significant increases in the annual hottest day temperatures (IPCC, 2023).

91 While global warming's impacts on other climatic variables, such as rainfall, involve
92 great uncertainty, there remains a substantial risk that precipitation may decrease or become
93 more variable in many sugarcane-producing regions in the future (Feng et al., 2013). Water
94 performs numerous critical functions in plants, with cooling through evaporation requiring the
95 largest volume of water. Thus, decreases in rainfall can exacerbate heat stress in plants by
96 effectively increasing the temperatures they experience (Inman-Bamber et al., 2012).
97 Consequently, accurate predictions of climate change impacts on sugarcane production depend
98 on robust modeling of how changes in temperature influence key plant physiological processes.

99 One of the advantages of sugarcane is its exceptional ability to use sunlight to drive
100 photosynthesis and produce biomass. The efficiency with which a crop converts canopy-
101 intercepted solar radiation into biomass can be quantified using a parameter known as radiation-
102 use efficiency (RUE, g MJ⁻¹) (Monteith et al., 1997). Sinclair and Muchow (1999) reported a
103 sugarcane RUE of about 2.0 g MJ⁻¹ and stated that this is the highest value of all economically
104 significant field crops. However, there is ongoing debate regarding whether RUE is a stable
105 trait across varieties and the growing season, excluding yield-limiting factors (Acreche, 2017;
106 Acreche et al., 2015; De Silva and De Costa, 2012; Dias et al., 2021a; Donaldson et al., 2008;
107 Robertson et al., 1996). This controversy reduces the accuracy of climate change predictions
108 on biomass production in different regions.

109 Resolving the RUE-variety debate requires some interpretation of how RUE is measured
110 and what different reported RUE values represent (see Table 1, which includes detailed
111 acronyms and their definition and units of measure). In principle, RUE is calculated as the
112 change in dry biomass between two points in time, divided by the solar radiation intercepted by
113 the crop during that period (Monteith et al., 1997). Typically, biomass measurements exclude
114 root biomass, and intercepted radiation can refer to either shortwave (global) (SRAD, MJ m⁻²
115 d⁻¹) or photosynthetically active radiation (PAR, MJ m⁻² d⁻¹). When RUE is calculated as the
116 total crop biomass at harvest (or final biomass sample) divided by total radiation intercepted
117 since crop start, it is referred to as 'apparent' RUE (RUE_A, g MJ⁻¹) (Robertson et al., 1996;
118 Sinclair and Muchow, 1999). Conversely, RUE calculated for a period between two biomass
119 sampling events is termed RUE_P (g MJ⁻¹). RUE_A can be lower than RUE_P if stresses (e.g., very
120 hot or cold conditions, drought, low nutrient availability) or other processes (high maintenance
121 respiration, lodging) reduce biomass accumulation rates during specific sampling periods. The
122 highest sugarcane RUE_P value for sugarcane in a single cropping season has been termed
123 RUE_{MAX} (g MJ⁻¹) (Jones et al., 2019; Muchow et al., 1994; Park et al., 2005; Robertson et al.,
124 1996; Sinclair and Muchow, 1999). For a large dataset, the highest RUE_{MAX} approaches the
125 theoretical maximum RUE for sugarcane (or a specific variety), referred to as RUE_O (Jones et
126 al., 2019; Singels, 2013).

127 RUE has been observed to be sensitive to air temperature (Dias et al., 2021a; Donaldson
128 et al., 2008). Crop species with the C₄ photosynthesis pathway, such as sugarcane, are better
129 adapted to higher temperatures (> 25 °C) compared to species with C₃ photosynthesis (Long,
130 1999). This adaptation underscores the importance of C₄ crop species in warmer future climatic
131 conditions. It is also acknowledged that C₄ crop species are significantly sensitive to variations
132 in air temperature within the 20–30 °C range (Long, 1999). This temperature range is typical of
133 current sugarcane-producing regions worldwide (Dias and Inman-Bamber, 2020). The
134 anticipated economic importance of sugarcane in the future underscores the urgent need to
135 predict the impacts of climate change on sugarcane productivity accurately. This is essential for
136 planning effective adaptation strategies to mitigate the adverse effects of climate change and,
137 where possible, capitalize on its positive impacts. In this context, RUE emerges as a critically
138 important physiological trait in sugarcane. The magnitude of expected future temperature
139 changes is substantial enough to significantly impact the RUE of typical C₄ crops by shifting
140 sugarcane-growing environments closer to, or further from, their optimal temperature range.

141 RUE is an important parameter in many dynamic sugarcane simulation models,
142 including DSSAT-CSM-CANEGRO (referred to as ‘DSSAT-Canegro’ from now on; Jones and
143 Singels, 2018) and APSIM-Sugar (referred as ‘APSIM’ from now on; Keating et al., 1999),
144 which are the most widely used worldwide to date (see Dias and Inman-Bamber, 2020 for a
145 complete list of sugarcane models). MOSICAS (Christina et al., 2021) and DSSAT-CSM-
146 SAMUCA (Vianna et al., 2020) have gained attention in the past five years. These models differ
147 in their representation of RUE_O and its response to temperature, which includes both the
148 cardinal temperature as well as the formalism for response to temperature (Jones et al., 2019;
149 Vianna et al., 2022) usually using linear (e.g. DSSAT-Canegro and APSIM) or symmetric
150 curvilinear (e.g. MOSICAS) responses. Some of these differences can be linked to the
151 difference in RUE representation in crop models, whether considering net (APSIM) or gross
152 (DSSAT-Canegro and MOSICAS) photosynthesis (Jones et al., 2021). To explore the impact of
153 climate change on sugarcane productivity, crop models are essential tools to represent biomass
154 accumulation response to temperature through the RUE concept, and literature suggests that
155 formalisms that represent the nonlinear and non-symmetric response of photosynthesis to
156 temperature (Johnson et al., 2010; Wang and Engel, 1998) can be used to improve the ability of
157 crop models to make reliable predictions under current or future climate scenarios (Wang et al.,
158 2017). Thus, having confidence in the sugarcane RUE response to temperature in these models
159 is critical.

160 The broad objective of this study was to characterize the sugarcane RUE response to
161 temperature using field data spanning environments and varieties across important sugarcane-
162 producing regions worldwide to ensure that predictions of future sugarcane yield are as accurate
163 and representative as possible. Specific objectives were to i) evaluate if RUE_{MAX} varies across
164 varieties in major producing countries, ii) assess whether the formalisms used in crop models
165 appropriately represent the RUE response to temperature, and iii) investigate the impact of
166 different formalisms on biomass predictions in crop models and their sensitivity to the choice
167 of RUE-temperature response, in the context of warming climates.

168 **2. Material & Methods**

169 **2.2. RUE Datasets**

170 The data used in this study included sugarcane in-field experimental data previously
 171 published in the literature (Table 2). Two experiment datasets were gathered: i) varietal
 172 experiment datasets, where experiments included variety comparisons in the same field, and ii)
 173 crop model calibration and sensitivity datasets, including only one variety per experiment. The
 174 first dataset was used to assess variety differences in RUE_{MAX} and RUE_A, and the second was
 175 used for crop model calibration and sensitivity analysis.

176 The “varietal experiment” dataset included measurements of the fraction of intercepted
 177 radiation (*f*iRAD) by the sugarcane canopy considering the incident global solar radiation
 178 (SRAD, in MJ m⁻² d⁻¹) and periodic aboveground dry mass (ADM, in tons, g or kg DM ha⁻¹)
 179 sampling over the crop season.

180 The “calibration and sensitivity” dataset included periodic ADM, *f*iRAD, and Leaf Area
 181 Index (LAI), except for South African data (SAF-PONG and SAF-MEDG), which only
 182 included observations of accumulated intercepted radiation with ADM. All experiments were
 183 fertilized under optimal conditions. Most of the experiments were irrigated except for a few,
 184 which were rainfed (experiments in Argentina and the RUN-SALS experiment in La Reunion)
 185 when rainfall was enough to meet sugarcane water demand. In this paper, a trial was defined as
 186 a one-year growth cycle in a specific site and country (Table 2).

187

188 **Table 2.** RUE datasets used for the varietal experiment analysis or the calibration and sensitivity
 189 analysis, including country, experiment identification, number (No.) of plant and ratoon crop
 190 cycles, and number of varieties compared in each site and data source.

Datasets	Country	Experiment ID	No. of Crop Cycle		No. of varieties	Source
			Plant	Ratoon		
Varietal experiment	La Reunion	RUN-DELI*	1	0	18	(Christina et al., 2020)
		RUN-ICSM*	1	1	5	(Jones et al., 2019)
	Brazil	BRA-MGSR*	2	0	6	(Dias et al., 2021a, 2020)
		BRA-PIGL*	3	0	6	(Dias et al., 2021a, 2020)
		BRA-CRU	1	1	3	(Cruz et al., 2021)
	South Africa	SAF-ICSM*	1	1	5	(Jones et al., 2019)
	USA	USA-ICSM*	0	1	6	(Jones et al., 2019)
	Zimbabwe	ZIM-ICSM*	1	0	6	(Jones et al., 2019)
Argentina	ARG-SAEZ	1	2	5	(Saez et al., 2019)	
Calibration & Sensitivity	La Reunion	RUN-SALS	0	3	R579	(Viaud, 2023)
		RUN-LINV	1	0		(Christina et al., 2020)
	Brazil	BRA-VIAN	0	2	RB867515	(Vianna et al., 2020)
		BRA-PIGL	3	0		(Dias et al., 2021a, 2020)
	South Africa	SAF-PONG	0	3	NCo376	(Donaldson, 2009)
		SAF-MEDG	0	2		(Singels et al., 2005)
Argentina	ARG-SAEZ	1	2	LCP 85-384	(Saez et al., 2019)	

191 * used in the variety x environment interaction analysis in this study (section 2.3)

192

193 2.3. Leaf photosynthesis and GPP datasets

194 In addition to RUE, in-field data of instantaneous leaf net photosynthesis (A_{net} , $\mu\text{mol m}^{-2}$
195 s^{-1}) and gross primary productivity (GPP, $\mu\text{mol m}^{-2} \text{s}^{-1}$) were gathered from the literature. A_{net}
196 and GPP variables were normalized between 0 and 1 using the 99% upper quantile as the higher
197 observed values. The sources, experimental conditions, and measurements are briefly described
198 below.

199 The first dataset measured leaf photosynthesis in sugarcane (plant crop cycle) in
200 Campinas, Sao Paulo State, Brazil (Magalhães Filho, 2014). The design included four varieties
201 (SP79-1011, IACSP94-2094, IACSP94-2101, and IACSP95-5000) with four replicates grown
202 under optimal fertilization and irrigation. A_{net} was measured on eleven dates, from 125 to 477
203 days after planting, from 7:00 to 17:00, every 2 hours. Measurements were taken using an
204 infrared gas analyzer (LI-6400XT, LICOR, Lincoln NE, USA) under natural variations of air
205 temperature, relative humidity and light intensity. Measurements were recorded under low
206 coefficient of variation ($CV < 5\%$) and temporal stability. Leaf and air temperature were
207 measured with the LI-6400XT. Note that leaf and air temperature were similar in this
208 experiment, and thus, the response to air temperature was chosen in the following analysis.

209 In the second dataset, GPP was estimated in a highly monitored rainfed experimental
210 site with eddy-covariance measurements during the second and third ratoons of sugarcane
211 variety SP83-2847 at an hourly time step, in Luiz Antonio, Sao Paulo State, Brazil (Cabral et
212 al., 2013, 2012). The filtered and gap-filled net ecosystem exchange (NEE) data was partitioned
213 into GPP and Ecosystem respiration (Reco) through the “nighttime partitioning” method
214 (Wutzler et al., 2018), applying the temperature response function of nighttime NEE fluxes to
215 estimate Reco during daytime, based on the Lloyd & Taylor model (Lloyd and Taylor, 1994).
216 GPP and air temperature above the canopy were used in our analysis.

217

218 2.4. RUE calculation and varietal effect analysis

219 RUE was calculated as the increase in sugarcane ADM divided by the accumulated daily
220 $iRAD$ in each plot from each trial. Two RUEs were calculated: RUE_A , defined as the final ADM
221 at harvest divided by the cumulated intercepted global radiation over the crop cycle since
222 planting, and RUE_{MAX} , calculated as the maximum RUE observed between successive biomass
223 sampling dates during the crop cycle. The corresponding mean air temperature to this RUE_{MAX}
224 was calculated as the mean between these two sampling dates. To calculate RUE, the daily
225 $fiRAD$ was estimated over the growth season based on a logistic growth function (Verhulst,
226 1838), a common sigmoidal-style curve used in agricultural studies (Archontoulis and Miguez,
227 2015):

$$228 \quad fiRAD(d) = \frac{fiRAD_{max}}{1 + 100 e^{-b d}} \quad (1)$$

$$229 \quad RUE_A = \frac{ADM(harvest)}{\sum_{d=0}^{d=harvest} fiRAD(d) SRAD(d)} \quad (2)$$

$$RUE_{MAX} = \max_{0 \leq d1, d2 \leq harvest} \left(\frac{ADM(d2) - ADM(d1)}{\sum_{d=d1}^{d=d2} fiRAD(d) SRAD(d)} \right) \quad (3)$$

Where d is the number of days since planting or previous harvest, $fiRAD_{max}$ is the maximum intercepted radiation reached, and b is an empirical fitting parameter.

Regressions were performed in each plot from the varietal experiment dataset using the *nlsLM* function (*minpack.lm* R package, Elzhov et al., 2016). A comparison between predicted $fiRAD$ and measured $fiRAD$ can be found in Supplementary Material Fig. S1, which yielded a root mean square error (RMSE) of 0.11 and a mean bias of -0.03.

First, the RUE response to the interaction between the variety and its environment (defined as a trial) was assessed using a subset of the varietal experiment where the same variety was tested in different sites (Table 2). The effect of the interaction between variety and trial, and crop class (CropClass, i.e., plant or ratoon crop) on RUE_A and RUE_{MAX} was assessed using a linear analysis of variance:

$$RUE \sim CropClass + Variety + Trial + CropClass:Variety + Trial:Variety \quad (4)$$

To ensure residue normality, the RUE variables were transformed using a Box-Cox transformation (*powerTransform* and *bcPower* R function, *car* R package, Fox et al., 2023). As non-significant interaction was found (see 3.1 result section), the influence of crop class and variety on the whole varietal experiment dataset was assessed using a mixed linear analysis of variance with the trial as a random effect (*nlme* R package, Pinheiro et al., 2022):

$$RUE \sim CropClass + Variety + (1|Trial) \quad (5)$$

Variables were also Box-Cox transformed to ensure residue normality. Predicted means and confidence intervals per variety or CropClass were estimated using the *emmeans* function (*emmeans* R package, Lenth et al., 2023). The *emmeans* function was also used to perform pairwise comparison with a Tukey p -adjustment method.

253

2.5. Description of RUE - temperature formalisms in crop models

In most sugarcane crop models, the influence of daily mean temperature (T_{MEAN}) on RUE is applied as an efficiency response function of temperature (fT_{RUE} , 0-1), and the daily potential biomass production results from fT_{RUE} , total intercepted radiation, and RUE_{MAX} . Crop models use different formalisms of temperature effects on RUE, and four of them were compared in this study. The first formalism (referred to as ApsimCanegro), used in the APSIM (Keating et al., 1999) and DSSAT-Canegro (Jones and Singels, 2018) models, consists of a trapezoidal function, with a linear increase or decrease between two optimal temperatures:

$$if(T_{MEAN} \leq T_B | T_{MEAN} \geq T_X) \{fT_{RUE} = 0\} \quad (6)$$

$$if(T_{MEAN} \geq T_{OPT1} | T_{MEAN} \leq T_{OPT2}) \{fT_{RUE} = 1\} \quad (7)$$

$$if(T_{MEAN} > T_B | T_{MEAN} < T_{OPT1}) \left\{ fT_{RUE} = \frac{T_{MEAN} - T_B}{T_{OPT1} - T_B} \right\} \quad (8)$$

265
$$if(T_{MEAN} > T_{OPT2} | T_{MEAN} < T_X) \left\{ fT_{RUE} = \frac{T_X - T_{MEAN}}{T_X - T_{OPT2}} \right\} \quad (9)$$

266 Where T_B , T_{OPT1} , T_{OPT2} , T_X are base, first, and second optimum (optimum range), and maximum
267 temperature, respectively.

268 The second formalism (referred to as Mosaic), used in the MOSICAS crop model
269 (Christina et al., 2021), was a symmetric curvilinear response with only one optimal
270 temperature and no base and maximum temperature but a rate of decrease with suboptimal
271 temperatures:

272
$$fT_{RUE} = 1 - T_{DEC} |T_{MEAN} - T_{OPT}|^\gamma \quad (10)$$

273
$$if(fT_{RUE} \leq 0) \{fT_{RUE} = 0\} \quad (11)$$

274 Where T_{OPT} is the optimal temperature and T_{DEC} and γ are parameters controlling the rate of
275 decrease in RUE with temperature.

276 The third formalism (referred to as Wang-Engel) proposed by (Wang and Engel, 1998)
277 has been shown to be effective in simulating the phenology and photosynthesis response of
278 varied annual crops to temperature (Streck et al., 2007; Wang et al., 2017, 2018). It is a non-
279 symmetric curvilinear response with an optimal temperature, base temperature, and maximum
280 temperature:

281
$$if(T_{MEAN} \leq T_B | T_{MEAN} \geq T_X) \{fT_{RUE} = 0\} \quad (12)$$

282
$$if(T_{MEAN} > T_B | T_{MEAN} < T_X) \left\{ \begin{array}{l} \alpha = \frac{\ln(2)}{\ln\left(\frac{T_X - T_B}{T_{OPT} - T_B}\right)} \\ fT_{RUE} = \left(\frac{2(T_{MEAN} - T_B)^\alpha (T_{OPT} - T_B)^\alpha - (T_{MEAN} - T_B)^{2\alpha}}{(T_{OPT} - T_B)^{2\alpha}} \right)^\beta \end{array} \right\} \quad (13)$$

283 Where T_{OPT} is the optimal temperature, T_B and T_X are the base and maximum temperature for
284 RUE, and β is a parameter controlling the curvature.

285 The fourth formalism (referred to as Johnson), a modified beta function to describe the
286 photosynthesis response to temperature, proposed by Johnson et al. (2010), was similar to the
287 Wang-Engel formalism but with a maximum threshold:

288
$$fT_{RUE} = \left(\frac{(1+c)T_{OPT} - T_B - c T_{MEAN}}{(1+c)T_{OPT} - T_B - c T_{REF}} \right) \left(\frac{T_{MEAN} - T_B}{T_{TREF} - T_B} \right)^c \quad (14)$$

289 Where T_{OPT} and T_{REF} are optimal temperatures, T_B is the base temperature, and c a curvature
290 coefficient.

291

292 2.6. Temperature response regression analysis

293 The parameterization of the f_{TRUE} functions was performed based on a quantile
294 regression to assess the envelop curve of RUE response to temperature, as many other processes
295 could reduce RUE_{MAX} other than temperature in the dataset, such as variation in water and
296 nutritional status in field-grown plants even under well-managed conditions. The dataset used
297 to assess the change in RUE_{MAX} with air temperature included the dataset used in the varietal
298 experiment (averaged per variety and trial, Table 1) as well as additional RUE_{MAX} values
299 published in the literature (Araújo, 2016; Barbosa, 2017; De Silva and De Costa, 2012;
300 Donaldson, 2009; Donaldson et al., 2008; Muchow et al., 1997; Olivier et al., 2016; Park et al.,
301 2005; Schwerz et al., 2018; Silva, 2009; Singels and Smit, 2002). To parameterize the f_{TRUE}
302 response, a normalized RUE_{MAX} was defined as the measured RUE_{MAX} divided by the
303 maximum predicted RUE_{MAX} obtained in the varietal effect analysis (i.e., 3.0 g DM MJ^{-1}).

304 Despite including published RUE data, the dataset did not include RUE_{MAX} response to
305 very high (above $32 \text{ }^\circ\text{C}$) or very low (below $15 \text{ }^\circ\text{C}$) air temperatures and could not be used alone
306 to parameterize RUE response to very low and high temperatures. Consequently, the change in
307 leaf photosynthesis and canopy GPP to temperature was also explored through two additional
308 datasets as a proxy for crop RUE (see section 2.2). The change in A_{net} and GPP with air
309 temperature was parameterized for each formalism using a 99% quantile regression (*nlrq*
310 function from *quantreg R* package, Koenker, 2009). For formalisms including a minimum
311 temperature, a lower boundary was defined for minimum temperature as $7 \text{ }^\circ\text{C}$ in the regression,
312 based on previous studies on canopy GPP or net ecosystem exchange responses to temperature
313 (Colmanetti et al., 2024; Cuadra et al., 2012) as well as leaf photosynthesis response (Peixoto
314 and Sage, 2017; Sage et al., 2013).

315 For high-temperature response, two strategies were defined for RUE response to air
316 temperature: i) a Leaf-type response, where temperature parameters at high temperatures
317 (T_{OPT2} , T_{MAX} , and T_{REF}) were fixed to the same value obtained in the leaf photosynthesis
318 response regression, and ii) a GPP-type response, in which the temperature parameters at high
319 temperatures were fixed to the same value obtained in the GPP regression. Note, as the Mosaic
320 formalism did not require minimum and maximum temperatures, no parameters were fixed for
321 this formalism. The change in RUE_{MAX} with mean air temperature in each formalism was
322 parameterized using a 90% quantile regression due to a lower number of observations ($n = 179$)
323 compared to A_{net} ($n = 1,055$) or GPP ($n = 8,436$).

324 To compare formalisms and assess the quantile regression quality, we calculated the
325 quantile loss (or pinball loss) index QLI as follows:

$$326 \quad \text{QLI} = \frac{1}{n} \sum_{i=1}^n \begin{cases} \tau (y_i - \hat{y}_i) & \text{if } (y_i \geq \hat{y}_i) \\ (1 - \tau) (y_i - \hat{y}_i) & \text{if } (y_i < \hat{y}_i) \end{cases} \quad (15)$$

327 Where y_i is the observation, \hat{y}_i is the corresponding predicted quantile, τ is the quantile level
328 (e.g., 0.9), and n is the number of observations. A lower QLI indicated a better quantile fit (note
329 that only comparison at the same quantile level is appropriate).

330 The default RUE parameterization for the different formalisms referred to the parameter
331 values obtained from the literature (Jones et al., 2021 for ApsimCanegro; Christina et al., 2021
332 for Mosicas; Wang et al., 2018 with maize parameters for Wang-Engel; Johnson et al., 2010
333 with C₄ species parameters and T_{OPT} = 33 °C for Johnson) and QLI was calculated for this
334 default parameterization.

335

336 2.7. Crop model sensitivity to RUE-T formalism and parameterization

337 The influence of model formalism and parameterization on RUE_A and ADM predictions
338 was explored in different locations under current and future climates. To this aim, we adapted
339 the MOSICAS crop model (Christina et al., 2021), which was written in R in open-access
340 (<https://gitlab.cirad.fr/mathias.christina/mosicas>), and thus the RUE – temperature response
341 equation was easily changed. MOSICAS, a deterministic thermoradiative type model that
342 accounts for water stress, consists of daily growth and carbon balance modules linked to a water
343 balance module. The canopy is represented by LAI following a ‘big-leaf’ approach, whereas
344 the intercepted radiation is calculated based on the extinction coefficient approach. The model
345 converts the daily intercepted radiation into daily gain in total dry mass, considering
346 temperature-reducing factors, water stress, and maintenance respiration. To use the
347 aboveground RUE measured in this study, we modified the model to express RUE based on
348 SRAD. Note that the MOSICAS model uses the air temperature above the canopy in the RUE
349 temperature response curve, so the input temperature from the weather station is directly used
350 in the calculation.

351 For each variety (Table 2, calibration and sensitivity analysis dataset) and depending on
352 available observations, we first calibrated the model on the dynamics of leaf area index (LAI),
353 fraction of intercepted radiation (*f*iRAD), or cumulated intercepted radiation (*i*RAD_c, details
354 on calibrated parameter in Supplementary Material Table S1). The RUE_{MAX} value was assumed
355 constant across varieties and fixed to the same higher value as the one used to normalize
356 RUE_{MAX} (3.0 g DM MJ⁻¹, see section 2.6). Parameter optimizations were performed using the
357 *RGenoud* optimization code provided with the MOSICAS model (see *gitlab* repository). Then,
358 we changed the RUE temperature response equations using the new parameter values obtained
359 during the procedure described in section 2.4. In addition, the sensitivity of each variety to water
360 stress was calibrated to simulate ADM observations accurately. RUE_A simulation accuracy was
361 assessed by comparing observations (calculated in section 2.5) and predictions based on relative
362 RMSE (rRMSE).

363 We assessed the long-term sensitivity of the crop model to the choice of formalism in
364 three sites on Reunion Island with contrasting temperature patterns. We chose Reunion Island
365 as a study case due to its high climate variability with sugarcane ranging from sea level to 1,000
366 m a.s.l. (Christina et al., 2021). Climate change scenarios are available at a high spatial
367 resolution (3x3 km, Leroux et al., 2021) for Reunion Island, and we used climate change data
368 from the RCP 8.5 scenarios to illustrate the sensitivity to high changes in temperature over time.
369 Based on a previous climate change study on sugarcane yield (Christina et al., 2024b), we

370 selected three sites with contrasting average annual temperatures (12.7, 22.1, and 25.1°C,
371 average over the 2016-2025 period) but similar average daily global radiation (8.6, 9.4, and 8.7
372 MJ m⁻² d⁻¹). These sites were located (latitude/longitude) at -20.93/55.66, -21.11/55.75, and -
373 21.14/55.72 at 20, 135, and 730 m a.s.l. Simulations were performed following the method
374 applied by Christina et al. (2024b) in these areas using the R579 variety. Potential ADM under
375 non-limiting water conditions was simulated to isolate the predicted ADM's response to the
376 temperature increase.

377

378 3. Results

379

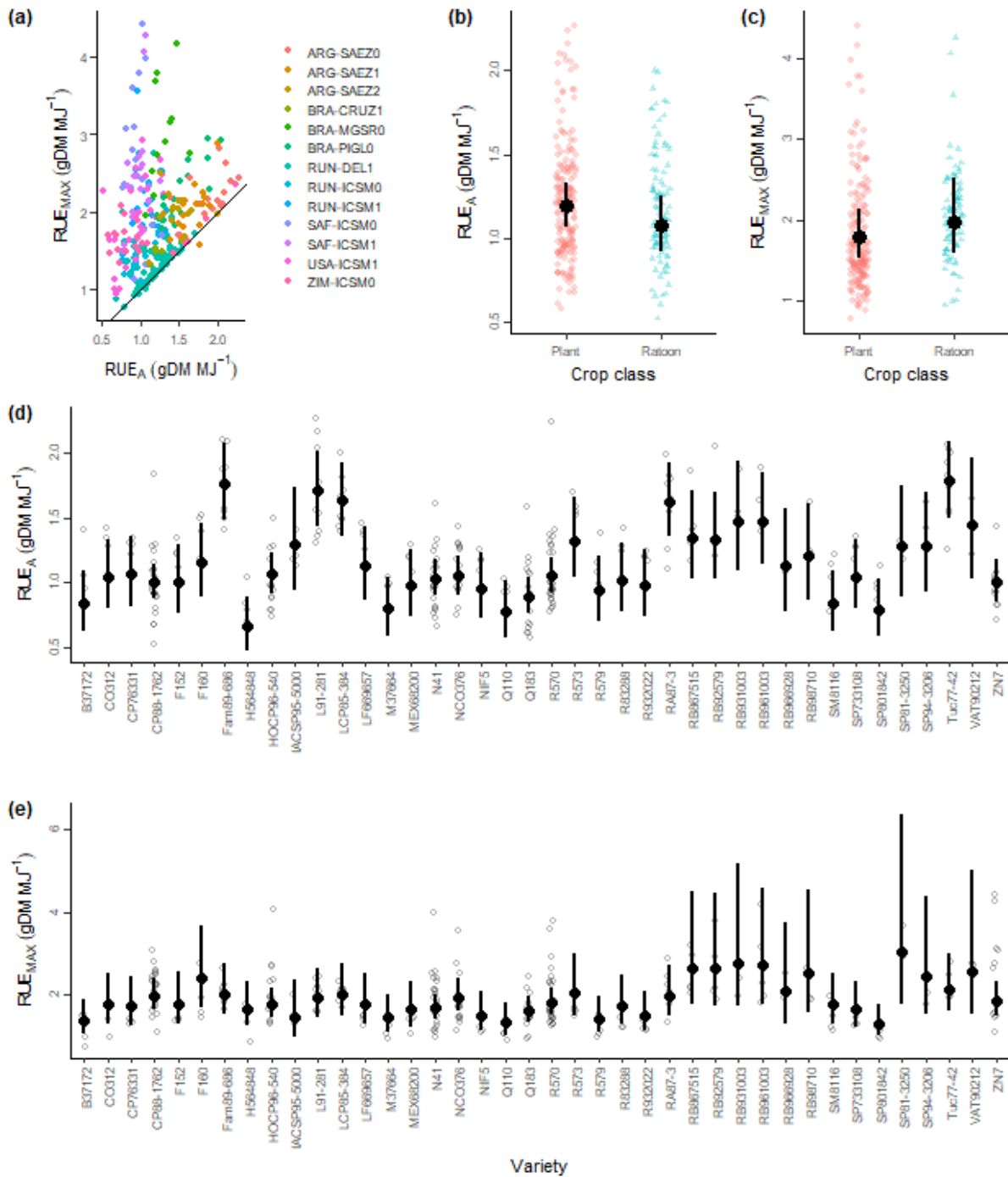
380 3.1. RUE response to variety and crop cycle

381 The maximum and apparent RUE showed high variability depending on countries, sites
382 and varieties with RUE_A values ranging from 0.5 to 2.5 g DM MJ⁻¹ and RUE_{MAX} ranging from
383 1.0 to 4.5 g DM MJ⁻¹ (Fig. 1a). In our varietal experiment dataset, there was no interaction
384 between variety and trial for RUE_A ($F_{21,141} = 1.06$; $p = 0.398$) or RUE_{MAX} ($F_{21,141} = 0.88$; $p =$
385 0.613). Similarly, neither RUE_A ($F_{10,141} = 0.78$; $p = 0.644$) nor RUE_{MAX} ($F_{10,141} = 1.26$; $p =$
386 0.258) presented interaction between crop class and variety. In the mixed model without
387 interaction, the crop class did not influence RUE_A ($F_{1,11} = 0.14$; $p = 0.71$) or RUE_{MAX} ($F_{1,11} =$
388 0.004 ; $p = 0.95$, Fig. 1b,c). On the contrary, RUE_A ($F_{39,236} = 3.08$; $p < 0.0001$) and, to a lesser
389 extent, RUE_{MAX} ($F_{39,236} = 1.54$; $p = 0.027$) differed between varieties.

390 Considering RUE_A , and crossed confidence intervals, a high number of significant
391 differences were noticed among varieties, with mean predicted values ranging from 0.66 to 1.78
392 g DM MJ⁻¹ (Fig. 1d). The highest RUE_A values were observed in varieties from Argentina (e.g.,
393 Fam, L91, RA or Tuc varieties) and Brazil (RB varieties). The change in RUE_{MAX} among
394 varieties was much lower compared to RUE_A . The mean RUE_{MAX} predicted values ranged from
395 1.32 to 3.04 g DM MJ⁻¹ (Fig. 1e). Nonetheless, considering pairwise regressions, only two
396 varieties differed among themselves in the RUE_{MAX} pairwise comparison at 5%, the SP80-1842
397 and F160 varieties ($p = 0.0491$). All others showed no significant differences in the pairwise
398 comparisons.

399

400



401
 402 **Fig. 1.** Apparent (RUE_A) and maximum (RUE_{MAX}) radiation use efficiency ($g\ DM\ MJ^{-1}$)
 403 depending on trials in the varietal experiment dataset (a), crop class (plant or ratoon crop, b, c),
 404 and variety (d, e). Black points and bars represent the predicted means and confidence interval
 405 by the mixed model. Small transparent points indicate the observed values.

406

407 **3.2. Change in RUE with temperature**

408 Based on the current default RUE formalism parameterizations (default temperature
 409 response parameter values), ApsimCanegro and Mosaic formalisms did not allow an
 410 appropriate envelop curve of normalized RUE_{MAX} response to mean air temperature with high
 411 quantile loss index (QLI, Fig. 2a, Table 3). ApsimCanegro and Mosaic overestimated RUE_{MAX}
 412 for temperatures ranging from 10 to 20 °C (Fig. 2a). Considering the net photosynthesis (A_{net})
 413 response at leaf level or GPP response to air temperature, all formalisms were able to accurately
 414 represent the observed values range with low 99% QLI ranging from 0.0055 to 0.0057 for A_{net}
 415 and 0.0061 to 0.0065 for GPP (Fig. 2b,c Table 3). Based on a visual assessment, the Johnson
 416 formalism represented a slightly lower increase in GPP for temperatures ranging from 10 to 20
 417 °C compared to other formalisms. Based on A_{net} and GPP regressions, we have fixed the base
 418 (T_B) and high temperature (T_X, T_{OPT2}, or T_{REF}) parameters in ApsimCanegro, Wang-Engel, and
 419 Johnson formalisms to propose two options based on the leaf photosynthesis or GPP dynamics
 420 at very high temperature (Fig. 2d,e, Table 2). In the normalized RUE_{MAX} – temperature
 421 response, whether based on A_{net} or GPP dynamics, all formalisms presented similar QLI, lower
 422 than the default parameterization (Table 3). Nonetheless, the Mosaic formalism failed to
 423 predict realistic base temperature in the GPP-type regression.

424

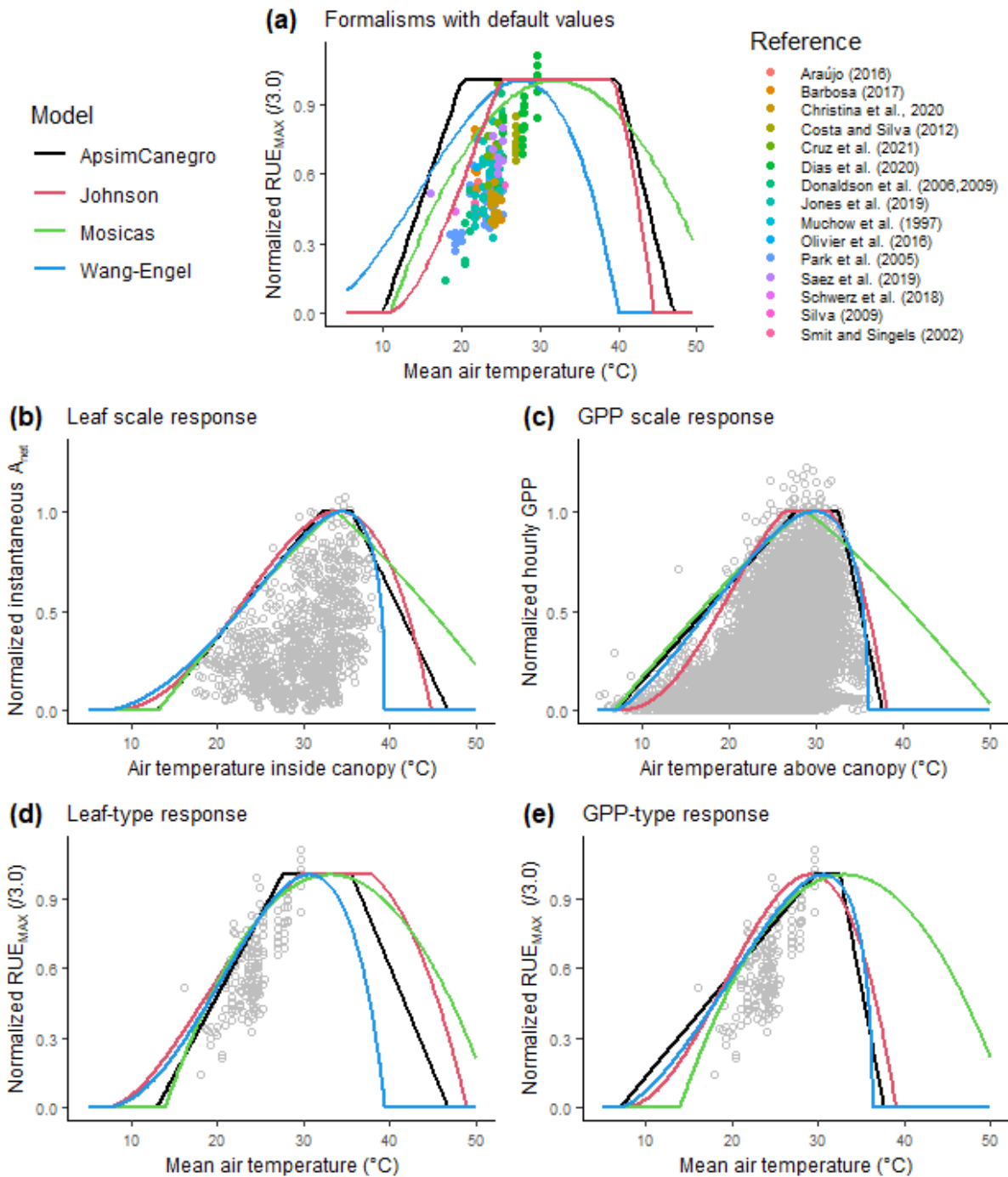
425 **Table 2.** Parameter values in the different RUE_{MAX} – temperature response formalisms
 426 depending on the quantile regressions on net leaf photosynthesis (A_{net}), gross primary
 427 productivity (GPP), and radiation use efficiency (RUE).

Formalism	Parameter	A _{net}	GPP	RUE _{MAX} (default)	RUE _{MAX} (Leaf-type)	RUE _{MAX} (GPP-type)
ApsimCanegro	T _B	13.0	7.0	10	13.0*	7.0*
	T _{OPT1}	32.1	27.6	20	27.8	29.6
	T _{OPT2}	35.6	32.6	40	35.6*	32.6*
	T _X	46.8	37.7	47	46.8*	37.7*
Mosaic	T _{OPT}	33.7	28.7	32	33.1	33.1
	T _{DEC}	0.032	0.027	0.0025	0.0027	0.0027
	γ	1.14	1.17	2.0	2.0	2.0
Wang-Engel	T _B	7.0	7.0	0	7.0*	7.0*
	T _{OPT}	34.5	29.9	27.5	30.7	30.6
	T _X	39.4	36.0	40	40.6*	36.0*
	β	0.39	0.44	1	0.84	0.44
Johnson	T _B	7.0	7.0	10	7.0*	7.0*
	T _{OPT}	33.4	26.4	25	29.6	29.1
	T _{REF}	34.0	29.1	33	34.0*	29.1*
	c	2.50	2.45	2	1.80	2.21

428 * fixed values in the regression.

429

430



431

432 **Fig. 2.** Change in normalized maximum radiation use efficiency (RUE_{MAX}) with mean air
 433 temperature depending on formalism (ApsimCanegro, Johnson, Mosicas, and Wang-Engel)
 434 based on default parameters values (a) and quantile regression using a Leaf-type (d) or GPP-
 435 type response (e) for very high and very low temperatures. Leaf-type and GPP-type response
 436 parameters for very low and high temperatures were obtained from the change in normalized
 437 net leaf photosynthesis (A_{net} , b) or normalized gross primary productivity (GPP, c) with
 438 temperature.

439

440

441 **Table 3.** Quantile loss index (QLI) in the different RUE_{MAX} – temperature response formalisms
 442 depending on the quantile regressions on net leaf photosynthesis (A_{net}), gross primary
 443 productivity (GPP), and radiation use efficiency (RUE). The quantiles used for regressions were
 444 0.99, 0.99, and 0.9 for A_{net} , GPP, and RUE due to differences in number of observations.

Formalism	Index	A_{net}	GPP	RUE (default)	RUE (Leaf-type)	RUE (GPP-type)
ApsimCanegro	QLI	0.00551	0.00613	0.0411	0.0248	0.0238
Mosicas	QLI	0.00570	0.00626	0.0280	0.0249	0.0249
Wang-Engel	QLI	0.00549	0.00628	0.0357	0.0242	0.0241
Johnson	QLI	0.00554	0.00646	0.0313	0.0240	0.0272

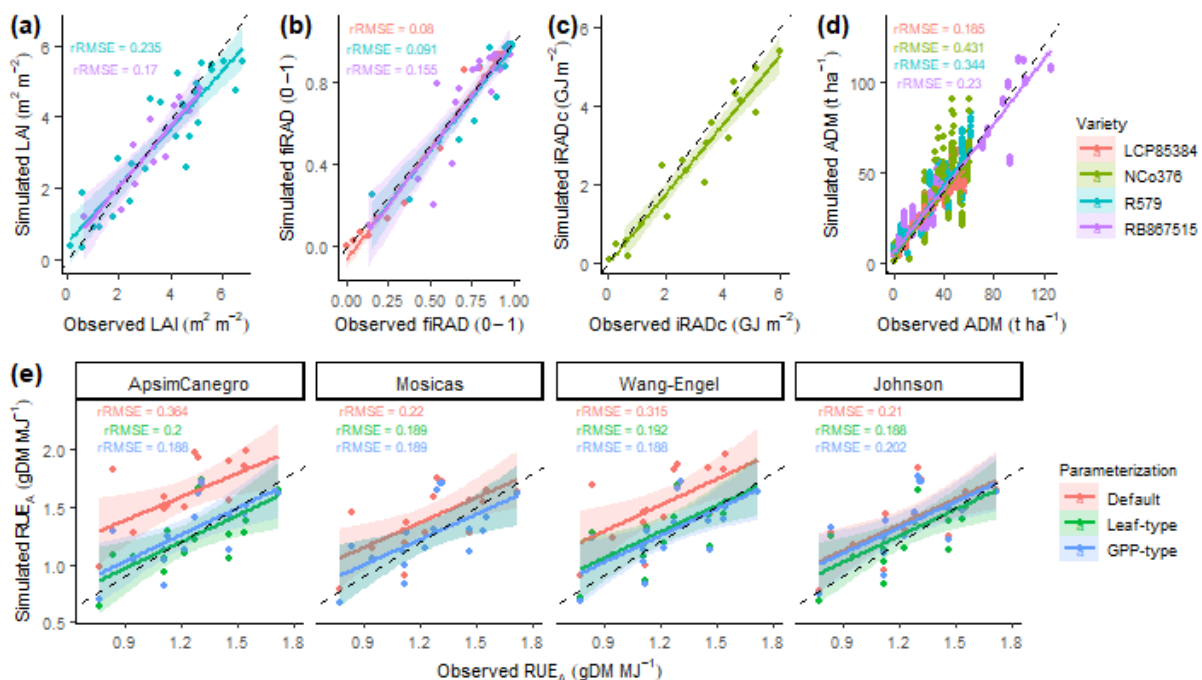
445

446

447 **3.3. Change in RUE_A simulations depending on formalism and parameterization**

448 Dynamics of LAI, fraction of intercepted radiation (*fi*RAD), and cumulative intercepted
 449 radiation were calibrated for each variety, allowing accurate prediction of *fi*RAD with rRMSE
 450 ranging from 0.08 to 0.16 depending on varieties (Fig. 3). Different parameters were calibrated,
 451 including a parameter controlling the daily rate of increase in LAI, the sensitivity of LAI to
 452 water stress and the extinction coefficient (Table S1). A unique optimal RUE_{MAX} value was
 453 used for all varieties (3.0 g DM MJ⁻¹), based on the maximum predicted value per variety in the
 454 variance analysis (Fig. 1) and used to normalize the RUE – temperature response (Fig. 2).
 455 Nonetheless, to accurately simulate the aboveground dry mass dynamics, the sensitivity of RUE
 456 to water stress was calibrated for each variety and lowered for LCP85384 and NCo376 varieties
 457 (Fig. 3d, Table S1). With a unique RUE_{MAX} across varieties, simulated aboveground dry
 458 biomass (ADM) rRMSE ranged from 0.19 to 0.43 (considering all formalism and
 459 parametrization combined, Fig. 3d). Nonetheless, the choice of formalism and parameterization
 460 influenced the accuracy of simulated RUE_A (Fig. 3e). Using the default parameterization, the
 461 ApsimCanegro, Mosaicas, and Wang-Engel formalisms tended to overestimate RUE_A values.
 462 For all four formalisms, the GPP-type and Leaf-type parameterization showed a lower rRMSE
 463 on RUE_A compared to default parameterization (Fig. 3e). In addition, GPP-type and Leaf-type
 464 parameterization showed similar rRMSE in the Mosaicas and Wan-Engel formalisms.
 465 Nonetheless, the GPP-type showed a slightly lower rRMSE (0.188) compared to Leaf-type
 466 parameterization (0.200) with ApsimCanegro, and it was the opposite for Johnson formalism.

467



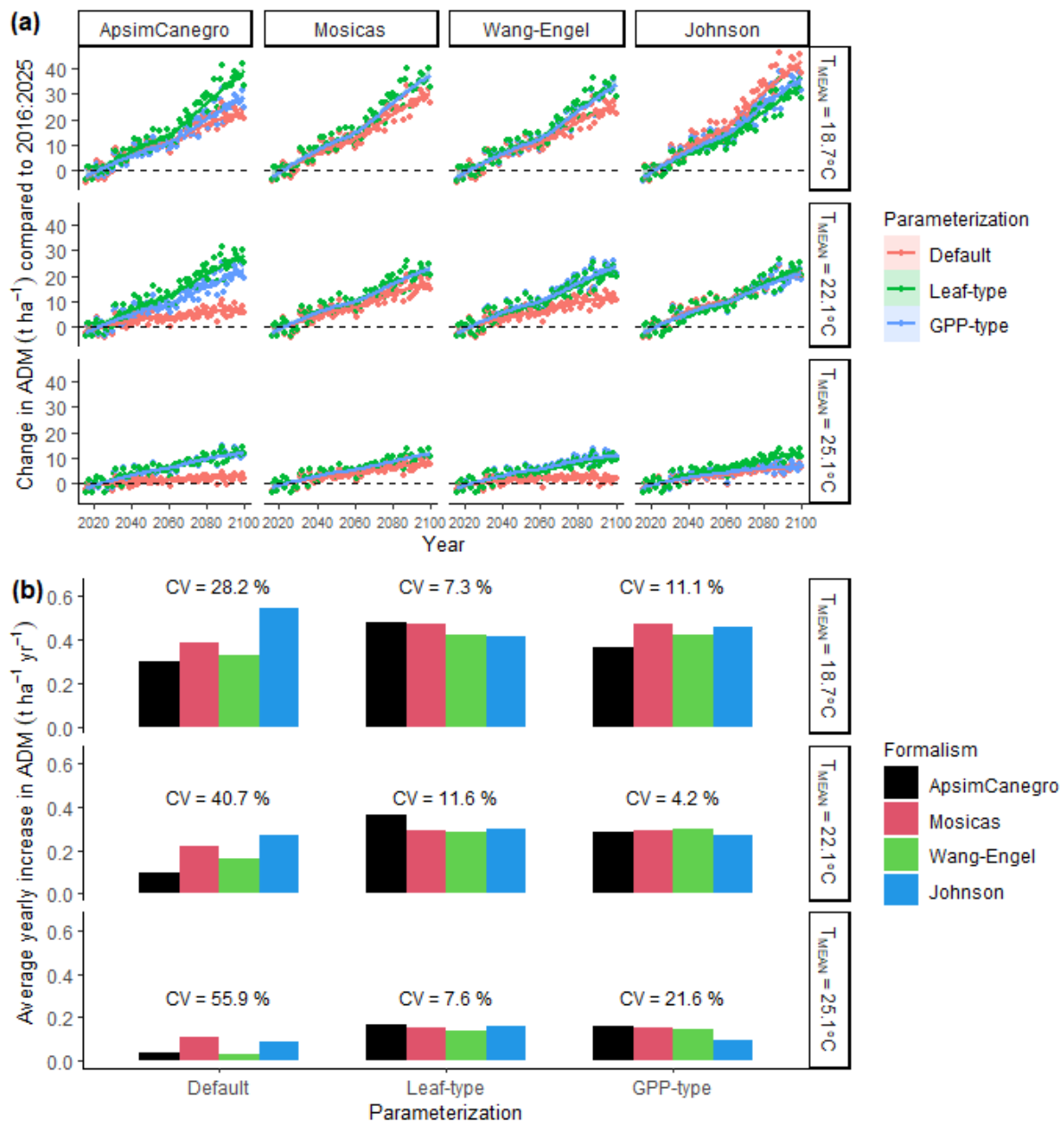
468

469 **Fig. 3.** Comparison between observed and simulated leaf area index (LAI, a), fraction of
 470 intercepted radiation (*fi*RAD, b), cumulated intercepted global radiation (*i*RADc, c),
 471 aboveground dry mass (ADM, d), and apparent radiation use efficiency (RUE_A, e) depending
 472 on the formalism used (ApsimCanegro, Mosaicas, Wang-Engel, and Jonhson) and the
 473 parameterization (Default, Leaf-type, and GPP-type). The relative rRMSE was indicated per
 474 variety or formalism parameterization. The dashed lines represent the identical curve (1:1).

475 **3.4. Biomass response to climate change and sensitivity to formalism**

476 The influence of model formalism choice and parameterization in model responses to
477 future climate was explored using three selected sites with contrasting mean air temperatures
478 in Reunion Island (Fig. 4), evaluated through projected potential ADM (without water stress).
479 Regarding parameterization, the change from the default parameterization to the new Leaf-type
480 or GPP-Type parameterization significantly affected the rate of increase in ADM over the years
481 in most sites (Fig. 4a). With the ApsimCanegro, Mosicas, and Wang-Engel formalisms, the
482 default parameterization predicted a lower increase in ADM over the years compared to the
483 new Leaf and GPP-Type parameterization. For example, with ApsimCanegro in the
484 intermediate site ($T_{\text{MEAN}} = 22.1 \text{ }^{\circ}\text{C}$), the average yearly increase in ADM was $0.09 \text{ t ha}^{-1} \text{ yr}^{-1}$
485 with the default parameterization. At the same time, it was 0.36 and $0.28 \text{ t ha}^{-1} \text{ yr}^{-1}$ with Leaf-
486 type and GPP-type parameterizations (Fig. 4b). In addition, the difference was higher in the
487 warmer site. With ApsimCanegro, the yearly increase in ADM was higher by 21, 200, and 307%
488 with the GPP-type parameterization compared to default one in the 18.7°C , 22.1°C , and 25.1°C
489 sites, respectively (Fig. 4b). Similar behavior was observed for the Wang-Engel formalism and
490 to a lesser extent the Mosicas formalism. With the Johnson formalism, lower differences
491 between default and new parameterization were observed, except in the coldest site, where the
492 increase in ADM was lower with the new parameterization than with the default one.

493 The sensitivity to the choice of formalism was low with the new parameterization
494 (whether Leaf-type or GPP-type) compared to the default parameterization (Fig. 4b). The
495 coefficient of variation (CV) in the yearly increase in ADM among formalisms was higher in
496 the default parameterization than the Leaf or GPP-type in all sites. Small differences were
497 observed between Leaf-type and GPP-type regarding sensitivity to the choice of formalism with
498 similar CV between 4.2% and 11.6% depending on sites, except for the GPP-type sensitivity in
499 the warmest site with a CV of 21.6% due to lower early increase with the Johnson formalism.



500

501 **Fig. 4.** Change in predicted potential sugarcane aboveground dry mass (ADM without water
 502 stress, $t\ ha^{-1}$) from 2015 to 2100 compared to the average 2016 to 2025 period (a) and average
 503 yearly increase in ADM (b) in three selected sites of Reunion Island with contrasted mean air
 504 temperatures ($T_{MEAN} = 18.7$, 22.1 , and $25.1\ ^{\circ}C$, respectively) and depending on model
 505 formalism and parameterization. The coefficient of variation (CV) of the yearly increase in
 506 ADM among formalism is indicated for each parameterization and site. Sugarcane growth was
 507 predicted under the RCP 8.5 climate change scenario.

508

509

510

511

512 4. Discussion

513

514 4.1. Contrasted response of RUE_A and RUE_{MAX} to variety

515 It is well known that sugarcane RUE declines with crop age, even when temperature,
516 water, and nutrient status are not apparently limiting. This phenomenon was termed the
517 ‘reduced growth phenomenon’ (RGP) by Park et al. (2005) and later on further explored by Van
518 Heerden et al. (2010). Our results suggest that the RUE before its decline, equivalent to
519 RUE_{MAX} , is minimally influenced by varieties, not only locally as observed in high-yielding
520 sites in Brazil (Dias et al., 2021a), but also for 40 varieties across six producing countries in our
521 study where only two varieties differed in RUE_{MAX} (SP80-1842 and F160). Sugarcane breeders
522 worldwide have likely involuntarily selected high RUE_{MAX} genotypes while screening for high
523 sucrose yields. Despite the expectation that RUE_{MAX} is closely linked to crop yield, existing
524 evidence does not always support this, likely due to RGP (De Silva and De Costa, 2012;
525 Donaldson et al., 2008; Jones et al., 2019). Our results highlight how RUE_A strongly differs
526 among varieties. Thus, there are opportunities to understand the reasons better and exploit that
527 for crop and agronomic intervention improvements to increase sugarcane production. As the
528 RGP varies among sugarcane varieties (Dias et al., 2021a), growth slowdown sensitivity could
529 explain differences in RUE_A despite similar RUE_{MAX} among varieties.

530 Lodging, declining leaf nitrogen status with age, localized feedback inhibition of
531 photosynthesis by high sugar content in leaf and/or high stalk sucrose content, and high
532 respiration were hypothesized to be the causes of RGP (Park et al., 2005; Van Heerden et al.,
533 2010) but none of them are conclusive to date and perhaps will not be because these phenomena
534 might have concomitant causes operating together to decrease RUE over time. Lodging is
535 definitely involved with RGP (Van Heerden et al., 2015), and recent studies showed how
536 lodging sensitivity differed significantly among varieties according to aerial traits as tillering
537 and plant height (Christina et al., 2024a) but also potentially to belowground traits
538 (Jongrunklang et al., 2018). However, there were many situations where crops did not lodge,
539 but RUE still declined towards harvest under unlimited growth conditions (Park et al., 2005;
540 Van Heerden et al., 2010).

541 Differences in RGP among varieties may represent differences in sensitivity to
542 environmental limitations when considering two key physiological processes - photosynthesis
543 and respiration. Leaf N status is closely linked to photosynthesis, and previous studies suggest
544 that as the sugarcane canopy begins to expand, the plant relies significantly on its internal
545 nitrogen reserves (Sage et al., 2013). As a result, the available nitrogen is distributed across a
546 larger leaf area, therefore declining A_{net} over time. However, evidence suggests that the nitrogen
547 use efficiency varies among sugarcane genotypes (Robinson et al., 2007), which has a close
548 relationship with photosynthesis as most leaf nitrogen is invested in photosynthetic proteins
549 such as Rubisco and PEPC (Sage et al., 2013). Alternatively, sugarcane photosynthesis can be
550 inhibited by the accumulation of sugars in leaves (McCormick et al., 2009, 2008, 2006). When
551 comparing the sensitivity of sugarcane to sucrose spraying – a way to inhibit photosynthesis,

552 there was a significant variation between genotypes when considering Rubisco and PEPC
553 abundances and activities (Ribeiro et al., 2017). In that regard, one could argue that other leaves
554 within the sugarcane canopy could compensate for the inhibitory effect of carbohydrates on the
555 photosynthesis of light-exposed leaves and prevent or even reduce a decline in overall canopy
556 photosynthesis (Inman-Bamber et al., 2011), a topic that deserves more research. In fact, leaf
557 photosynthesis in sugarcane is modulated more by the leaf carbohydrate dynamics than by leaf
558 carbohydrate concentration (Ribeiro et al., 2017). When active sinks demand energy and
559 carbon, leaf photosynthesis in sugarcane is stimulated (Ribeiro et al., 2017). In such a scenario,
560 high-yielding genotypes might present stronger sinks and higher stimulation of photosynthesis
561 compared to low-yielding genotypes. Taken together, these findings would suggest that the
562 extension of down- or up-regulation of photosynthesis by sugars is genotype-dependent and
563 could justify variations in RGP and RUE_A among sugarcane cultivars studied herein.

564 Regarding respiration and its components, the scientific literature is very limited when
565 considering its importance in field-grown crops, such as sugarcane. For instance, both
566 maintenance and growth respiration would increase due to high temperatures (Amthor, 2025),
567 and literature suggests that increased biomass production for summer-started crops limits high
568 sugarcane yields compared to winter-started ones under well-watered and managed conditions,
569 possibly due to elevated maintenance respiration of larger crops (Van Heerden et al., 2010). As
570 the RGP occurs during the final months of the crop cycle during stalk maturation in dry and
571 cold winter seasons (Martins et al., 2025), one could argue that changes in respiration are not
572 key in determining RGP in tropical conditions. However, the same is not true when considering
573 photosynthesis, which is significantly reduced during winter and certainly reduces RUE_A in
574 sugarcane plants (Martins et al., 2024, 2025). Although there is a significant variation in leaf
575 respiration rate among sugarcane genotypes (Almeida et al., 2021; Ribeiro et al., 2017; Tejera
576 et al., 2007), the impact of such process on overall canopy respiration and then on RGP and
577 RUE_A of sugarcane remains unknown. Understanding this response is a crucial target for crop
578 improvement (Amthor, 2025).

579 In addition to RGP sensitivity, other processes could explain the difference in RUE_{MAX}
580 and RUE_A response to variety, such as the diffuse radiation effect (determining yield factor) or
581 the water stress sensitivity (limiting factor). RUE is well known to increase with the fraction of
582 diffuse radiation (Sinclair et al., 1992). Nonetheless, the extent to which different sugarcane
583 canopy architectures among varieties may induce different responses to diffuse radiation still
584 needs deeper investigation (Luo et al., 2014, 2013). Under water-limited conditions, there is
585 evidence that some varieties are better than others regarding water deficit tolerance (Inman-
586 Bamber and Smith, 2005; Venkataramana et al., 1986). Such differences in key periods of
587 sugarcane growth could explain why RUE_A may differ among varieties while RUE_{MAX} remains
588 constant. Nonetheless, previous studies on an extensive range of varieties showed that the
589 genotype x water stress interactions effect on stomatal conductance and yield were small
590 compared to the genotype effect (Basnayake et al., 2015, 2012), suggesting that differences in
591 water-stress resistance may not be a significant effect explaining the high difference in RUE_A .
592 In our study, most of the experiments were irrigated, so no or limited water stress should have

593 occurred, supporting the hypothesis that differences in RUE_A may be primarily linked to
594 differences in growth slowdown sensitivity (Dias et al., 2021a).

595

596 **4.2. RUE response to temperature**

597 Improving the temperature response in crop models is essential to reduce the uncertainty
598 of crop yield projections in the context of global warming (Maiorano et al., 2017; Wang et al.,
599 2017). Nonetheless, our study highlights that biomass production response to temperature is
600 more sensitive to the choice of cardinal temperatures (base, optimal, and maximum) than the
601 choice of formalism itself. In addition, improvements in the parameterization significantly
602 reduced the differences between models.

603 Based on our study, we recommend that crop models that use the daily RUE_O as a
604 parameter, a base temperature of 7 °C and optimal temperature ranging from 30 to 33 °C,
605 depending on formalisms, should be encouraged. This base temperature is lower than the ones
606 historically adopted to represent photosynthesis in the widely used sugarcane crop models (T_B
607 = 9 °C, APSIM, Keating et al., 1999; T_B = 10 °C, DSSAT-Canegro, Jones and Singels, 2018),
608 however it is consistent with carbon exchange measurements at the canopy (Colmanetti et al.,
609 2024; Cuadra et al., 2012) and leaf-scale photosynthesis (Peixoto and Sage, 2017; Sage et al.,
610 2013). Nevertheless, estimating the maximum mean daily temperature based on RUE_{MAX} is
611 difficult considering the usual sugarcane-cultivated regions since average temperature above
612 35°C is not observed in such areas. Therefore, obtaining the uppermost RUE_{MAX} temperature
613 response based on biomass accumulation will require experiments in controlled environments
614 or specific experiments under very warm regions.

615 With the currently available datasets, we recommend using GPP-type maximum
616 temperatures between 36 and 38°C for models based on air temperature above the canopy (e.g.,
617 DSSAT-Canegro, APSIM-Sugar, and MOSICAS) and using Leaf-type maximum temperatures
618 between 41 and 47 °C for models based on the air temperature inside the canopy (e.g., STICS,
619 Kebalo et al., 2025) depending on formalism. Nonetheless, for models that use a daily time
620 step, our study suggests that the maximum temperature adjustments are less sensitive since
621 those conditions are not common over regions where sugarcane is cultivated (neither nowadays
622 nor in the future). However, it should be important for models using photosynthesis at an hourly
623 scale (e.g., JULES, Vianna et al., 2022). Even if our study highlights a low sensitivity to the
624 choice of RUE-temperature formalism, we recommend Wang-Engel as a more appropriate
625 formalism for future studies, as i) the parameters have clearer meanings compared to Johnson
626 formalism, ii) the ApsimCanegro formalism was found to be highly sensitive to the cardinal
627 temperature values, compared to other formalisms, and iii) Mosicas does not allow a base
628 temperature to be specified.

629 Whether the RUE_O response to temperature may differ among varieties remains
630 unsolved in our analysis. The absence of interaction between variety and the trial on RUE_{MAX}
631 in our study suggests that varieties should respond similarly to temperature (as suggested by
632 Parent and Tardieu, 2012, in various crops). Previous studies on an international dataset also

633 showed low interaction between genotype and environments with stable RUE_O in four countries
634 (Jones et al., 2019). Nonetheless, previous studies at the leaf scale suggest that some sugarcane
635 varieties or species may differ in their photosynthetic rate response to chilling (Du et al., 1999)
636 or heat stress (Kohila and Gomathi, 2018; Liu et al., 2020; Peixoto and Sage, 2017). Currently,
637 we recommend fixing the cardinal temperature parameters for the sugarcane species,
638 independent of varieties and across environments. More detailed datasets may reveal that
639 RUE_{MAX} response to temperature significantly differs among varieties.

640 As highlighted by our study, the estimation of cardinal temperatures (base, optimal, and
641 maximum) for RUE has substantial consequences for application in climate change studies,
642 with potential underestimation of the increase in ADM in previous studies using the two most
643 used models APSIM-Sugar (e.g., Dias et al., 2021b) and DSSAT-Canegro (e.g., Marin et al.,
644 2013; Singels et al., 2014). While we are confident that our new parameterization should reduce
645 the uncertainty of ADM estimates for projected climate change, the current formalisms in crop
646 models still contain an inherent bias by not considering the daily temperature range (minimum
647 at night and maximum during the day). High temperatures at hourly time scales are strongly
648 correlated with low VPD and could reduce photosynthesis at midday and potentially daily RUE.
649 For example, a modeling approach using an hourly time scale model (JULES) simulated an
650 abrupt negative impact on sugarcane yields when daytime temperatures above 35°C become
651 more frequent in Brazil (Vianna et al., 2022). In addition, we cannot rule out the influence of
652 low night temperatures in reducing sugarcane photosynthesis, as reported in other species
653 (Santos et al., 2011). To overcome such limitations into current crop models, a first option would
654 be to develop hourly time-scale routines into crop models, but it becomes potentially more
655 difficult to use in climate change scenario assessments. A second option would be to use an
656 empirical weighting factor applied to the daily maximum temperature to account for changes
657 in VPD during the day. However, it may increase the level of empiricism in model
658 parametrization. Most importantly, an appropriate compromise has to be found between
659 biological reality and parsimony in crop models (Hammer et al., 2019; Yin et al., 2021).

660

661 **4.3. Recommendation for calibration strategy in crop models and varietal-sensitivity** 662 **improvements**

663 As discussed in the previous section, the first step in calibrating crop models is to
664 standardize the cardinal temperatures for sugarcane across all environments and varieties. If the
665 cardinal temperatures or formalisms are modified from previous model versions, it may
666 necessitate reparametrizing RUE_O in crop models. This does not imply that earlier studies were
667 incorrect, but rather that they may have used an inappropriate RUE_O (e.g., very high RUE in
668 Marin et al., 2011), or changed other parameter values (e.g., distinct extinction coefficient
669 among sites, Dias et al., 2021a, 2019), to compensate for underestimating the effect of
670 temperature.

671 This study used an RUE_O value of 3.0 g DM MJ⁻¹ using ADM and *iRAD*. While this
672 value might seem high, it was derived from trials conducted under optimal temperature and

673 irrigation conditions in Brazil. This value is higher than the ones used in previous studies
674 modeling sugarcane growth in South Africa, Zimbabwe, USA, Australia, or La Reunion, with
675 RUE_O ranging from 1.3 to 2.1 g DM MJ⁻¹ depending on crop models and varieties (Jones et al.,
676 2021; Thorburn et al., 2010), which were conducted under lower temperature conditions.
677 Nonetheless, our value is lower than the one used in modeling studies in Brazil with Canegro
678 in DSSAT v4.5 (Singels et al., 2010), with RUE_O values around 4.6 g DM MJ⁻¹ (Dias and
679 Sentelhas, 2017; Marin et al., 2015). Herein, the RUE_O chosen is directly linked to the dataset
680 used and may be subjected to biases, such as measurement errors or the absence of data from
681 even higher temperature conditions. This value can be used as a reference but the choice of the
682 RUE_O value must also consider the processes incorporated into carbon assimilation in crop
683 models (Table 3). This includes factors such as the type of radiation used (RAD vs. PAR),
684 whether the biomass considered includes above- and belowground components or only
685 aboveground, and whether maintenance respiration is considered before (net RUE) or after
686 (gross RUE) C assimilation.

687 As an initial approach, we recommend fixing the RUE_O across all environments.
688 However, while most models account for water stress, other processes influencing carbon
689 assimilation are not always included (Table 3). The processes not necessarily included in the
690 models are diverse: nitrogen stress, lodging and other RGP processes in high-yield
691 environments, unpredictable variations in the root-to-shoot ratio (which is highly influenced by
692 environmental factors, as highlighted by Chevalier et al., 2023), and for example the effects of
693 diffuse radiation. When the crop models do not consider these processes, it may be necessary
694 to calibrate the RUE_O for a homogeneous environment (in terms of soil and climate).
695 Nonetheless, modelers should remain aware that this calibration might inadvertently
696 compensate for other environmental factors the model cannot adequately represent.

697 Regarding varietal effects, our results suggest that RUE_O should be standardized across
698 varieties. Therefore, varietal calibration should focus on other processes that influence the daily
699 RUE calculation in crop models, as mentioned in the discussion on variety in section 4.1. Many
700 processes that vary among varieties are not currently accounted for in crop models or are
701 accounted for but not easily calibrated per variety (Table 3). In such cases, a varietal calibration
702 of RUE_O may be necessary with the same limits as previously mentioned. Nonetheless, to
703 effectively use these models as tools for evaluating varieties and potential adaptations to climate
704 change, it is essential to incorporate these processes in future crop model development,
705 especially for high-yielding varieties. For these high-yielding varieties, two key processes
706 warrant further investigation: i) integrating RGP mechanisms into crop models more
707 mechanistically, as suggested by Van Heerden et al. (2015) in Canegro structure, and ii)
708 assessing how respiration is incorporated into crop models, given its critical role and sensitivity
709 to varying temperature.

710

711

712 **Table 3.** Processes included in the RUE_o concept and daily RUE calculations in four crop
 713 models, and possibility to perform a varietal calibration on these processes.

		DSSAT- Canegro	APSIM	MOSICAS	STICS
Processes included in RUE _o	Biomass Radiation Respiration	whole PAR gross RUE	ADM RAD net RUE	whole PAR gross RUE	ADM + perennial reserve PAR net RUE
Processes accounted for in daily RUE calculation	Water stress Nitrogen stress Diffuse radiation effect Change in root-to-shoot Lodging RGP	yes no no yes yes no	yes yes no yes yes ¹ yes ¹	yes no yes yes no no	yes yes no yes no no
Possibility to perform a varietal calibration	Water stress sensitivity Nitrogen stress sensitivity Diffuse radiation effect Change in root-to-shoot Lodging RGP	yes no no no yes no	yes yes no yes yes ¹ yes ¹	yes no yes yes no no	yes yes no no no no

714 * RGP: reduce growth phenomenon; RAD: global radiation; PAR: photosynthetic active radiation; ADM:
 715 aboveground dry mass

716 ¹ See section '2.2.3. Reduced growth phenomenon (RGP)' in (Dias et al., 2019) for further details.

717

718 **5. Conclusion**

719 This study provides critical insights into sugarcane RUE, showing that RUE_{MAX} is stable
720 across elite varieties and is highly temperature-dependent, while RUE_A varies significantly.
721 Therefore, in crop modeling, RUE_{MAX} should be assumed constant across genotypes and
722 environments. Based on an international dataset, the analysis emphasizes the importance of
723 accurately parameterizing crop model formalisms and cardinal temperatures (optimal: 30–33
724 °C) to improve predictions of sugarcane yield under climate change. Additionally, it offers a
725 reference for calibrating RUE temperature response formalisms in major crop models and
726 provides guidelines for model calibration. While RUE_{MAX} remains consistent, the sensitivity of
727 RUE_A to environmental factors highlights the need for refining crop models to capture better
728 varietal responses to factors related to RGP (i.e., lodging, the decline in N use efficiency with
729 age, and respiration of large crops). Incorporating these mechanisms will enable crop models
730 to more accurately simulate sugarcane productivity dynamics, supporting climate impact
731 assessments and breeding programs for high-yield, climate-resilient varieties.

732

733 **CRedit authorship contribution statement**

734 **Mathias Christina:** Conceptualization; Data curation; Formal analysis; Methodology;
735 Project administration; Software; Visualization, Writing – original draft. **David Clark:** Data
736 curation; Methodology; Project administration. **Fabio Ricardo Marin:** Data curation;
737 Methodology; Project administration. **Rafael Vasconcelos Ribeiro:** Data curation;
738 Investigation. **Julio Victor Saez:** Data curation; Investigation. **Tendai Polite Chibarabada:**
739 Data curation; Investigation. **Murilo dos Santos Vianna:** Data curation; Investigation.
740 **Matthew Jones:** Methodology; Writing – original draft. **Santiago Vianna Cuadra:** Data
741 curation; Investigation. **Osvaldo Machado Rodrigues Cabral:** Data curation; Investigation.
742 **Martin Moises Acreche Acreche:** Investigation. **Henrique Boriolo Dias:** Conceptualization;
743 Data Curation; Investigation; Methodology; Project administration; Writing – original draft. **All**
744 **authors:** Writing – review & editing.

745

746 **Declaration of competing interest**

747 The authors declare that they have no known competing financial interests or personal
748 relationships that could have appeared to influence the work reported in this paper.

749

750 **Acknowledgements**

751 This study was supported by the International Consortium for Sugarcane Modelling
752 (ICSM) and its constituent organizations. The projects that funded the acquisition of
753 experimental data are described in each of the publications cited. Rafael V. Ribeiro is a fellow
754 of the National Council for Scientific and Technological Development (CNPq, Brazil, grant
755 304295/2022-1). Henrique B. Dias is grateful to the São Paulo Research Foundation (FAPESP),
756 which facilitated the early days of conceptualization and RUE literature review for this study
757 through the grants #2016/11170-2 and #2017/24424-5.

758

759 **Data availability**

760 Experimental datasets used in the analysis included open and restricted data. Details on
761 data availability were given in Supplementary Material. R scripts codes used to perform
762 analyses are available in open-source in a gitlab repository
763 ([https://gitlab.cirad.fr/mathias.christina/script_peerreviewedarticle/-](https://gitlab.cirad.fr/mathias.christina/script_peerreviewedarticle/-/tree/master/2025_XXX_ICSM_RUE?ref_type=heads)
764 [/tree/master/2025_XXX_ICSM_RUE?ref_type=heads](https://gitlab.cirad.fr/mathias.christina/script_peerreviewedarticle/-/tree/master/2025_XXX_ICSM_RUE?ref_type=heads)).

765

766

767 **Reference**

- 768 Acreche, M.M., 2017. Nitrogen-, water- and radiation-use efficiencies affected by sugarcane
769 breeding in Argentina. *Plant Breed.* 136, 174–181. <https://doi.org/10.1111/pbr.12440>
- 770 Acreche, M.M., Saez, J.V., Chalco Vera, J., 2015. Physiological bases of genetic gains in
771 sugarcane yield in Argentina. *Field Crops Res.* 175, 80–86.
772 <https://doi.org/10.1016/j.fcr.2015.02.002>
- 773 Almeida, R.L., Silveira, N.M., Pacheco, V.S., Xavier, M.A., Ribeiro, R.V., Machado, E.C.,
774 2021. Variability and heritability of photosynthetic traits in *Saccharum* complex. *Theor.*
775 *Exp. Plant Physiol.* 33, 343–355. <https://doi.org/10.1007/s40626-021-00217-x>
- 776 Amthor, J.S., 2025. After photosynthesis, what then: Importance of respiration to crop growth
777 and yield. *Field Crops Res.* 321, 109638. <https://doi.org/10.1016/j.fcr.2024.109638>
- 778 Araújo, R.M., 2016. Caracterização morfológica e respostas às condições agrometeorológicas
779 da cana-de-açúcar para o ambiente de Clima Temperado (PhD Thesis). Universidade
780 Federal de Pelotas, Pelotas, Brazil.
- 781 Archontoulis, S.V., Miguez, F.E., 2015. Nonlinear Regression Models and Applications in
782 Agricultural Research. *Agron. J.* 107, 786–798.
783 <https://doi.org/10.2134/agronj2012.0506>
- 784 Barbosa, A. de M., 2017. Ambiente de produção na eficiência da conversão de energia solar em
785 cultivares de cana-de-açúcar (PhD Thesis). Universidade Estadual Paulista, Botucatu,
786 Brazil.
- 787 Basnayake, J., Jackson, P.A., Inman-Bamber, N.G., Lakshmanan, P., 2015. Sugarcane for water-
788 limited environments. Variation in stomatal conductance and its genetic correlation with
789 crop productivity. *J. Exp. Bot.* 66, 3945–3958. <https://doi.org/10.1093/jxb/erv194>
- 790 Basnayake, J., Jackson, P.A., Inman-Bamber, N.G., Lakshmanan, P., 2012. Sugarcane for water-
791 limited environments. Genetic variation in cane yield and sugar content in response to
792 water stress. *J. Exp. Bot.* 63, 6023–6033. <https://doi.org/10.1093/jxb/ers251>
- 793 Cabral, O.M.R., Rocha, H.R., Gash, J.H., Ligo, M.A.V., Ramos, N.P., Packer, A.P., Batista,
794 E.R., 2013. Fluxes of CO₂ above a sugarcane plantation in Brazil. *Agric. For. Meteorol.*
795 182–183, 54–66. <https://doi.org/10.1016/j.agrformet.2013.08.004>
- 796 Cabral, O.M.R., Rocha, H.R., Gash, J.H., Ligo, M.A.V., Tatsch, J.D., Freitas, H.C., Brasilio, E.,
797 2012. Water use in a sugarcane plantation. *GCB Bioenergy* 4, 555–565.
798 <https://doi.org/10.1111/j.1757-1707.2011.01155.x>
- 799 Chevalier, L., Christina, M., Fevrier, A., Jourdan, C., Ramos, M., Poultney, D., Versini, A.,
800 2023. Sugarcane responds to nitrogen fertilization by reducing root biomass without
801 modifying root N accumulation, in: *Proceedings of the XXXI International Society of*
802 *Sugar Cane Technologists*. Presented at the XXXVI ISSCT Congress, ISSCT,
803 Hyderabad, India, pp. 212–220.
- 804 Christina, M., Chaput, M., Martiné, J.-F., Auzoux, S., 2020. ECOFI: a database of sugar and
805 energy cane field trials. *Open Data J. Agric. Res.* 6, 14–18.
806 <https://doi.org/10.18174/odjar.v6i0.16322>
- 807 Christina, M., Heuclin, B., Pilloni, R., Mellin, M., Barau, L., Hoarau, J.-Y., Dumont, T., 2024a.
808 Climate, altitude, yield, and varieties drive lodging in sugarcane: A random forest
809 approach to predict risk levels on a tropical island. *Eur. J. Agron.* 161, 127381.
810 <https://doi.org/10.1016/j.eja.2024.127381>
- 811 Christina, M., Jones, M.-R., Versini, A., Mézino, M., Le Mézo, L., Auzoux, S., Soulié, J.C.,
812 Poser, C., Gérardaux, E., 2021. Impact of climate variability and extreme rainfall

813 events on sugarcane yield gap in a tropical Island. *Field Crops Res.* 274, 108326.
814 <https://doi.org/10.1016/j.fcr.2021.108326>

815 Christina, M., Mézino, M., Le Mezo, L., Todoroff, P., 2024b. Modeled Impact of Climate
816 Change on Sugarcane Yield in Réunion, a Tropical Island. *Sugar Tech* 26, 639–646.
817 <https://doi.org/10.1007/s12355-024-01372-6>

818 Colmanetti, M.A.A., Cuadra, S.V., Lamparelli, R.A.C., Cabral, O.M.R., de Castro Victoria, D.,
819 de Almeida Monteiro, J.E.B., de Freitas, H.C., Galdos, M.V., Marafon, A.C., de Andrade
820 Junior, A.S., 2024. Modeling sugarcane development and growth within ECOSMOS
821 biophysical model. *Eur. J. Agron.* 154, 127061.

822 Cruz, L.P., Pacheco, V.S., Silva, L.M., Almeida, R.L., Miranda, M.T., Pissolato, M.D.,
823 Machado, E.C., Ribeiro, R.V., 2021. Morpho-physiological bases of biomass production
824 by energy cane and sugarcane: A comparative study. *Ind. Crops Prod.* 171, 113884.
825 <https://doi.org/10.1016/j.indcrop.2021.113884>

826 Cuadra, S.V., Costa, M.H., Kucharik, C.J., Da Rocha, H.R., Tatsch, J.D., Inman-Bamber, G.,
827 Da Rocha, R.P., Leite, C.C., Cabral, O.M.R., 2012. A biophysical model of Sugarcane
828 growth. *GCB Bioenergy* 4, 36–48. <https://doi.org/10.1111/j.1757-1707.2011.01105.x>

829 De Silva, A.L.C., De Costa, W.A.J.M., 2012. Growth and Radiation Use Efficiency of
830 Sugarcane Under Irrigated and Rain-fed Conditions in Sri Lanka. *Sugar Tech* 14, 247–
831 254. <https://doi.org/10.1007/s12355-012-0148-y>

832 Dias, H.B., Inman-Bamber, G., 2020. Sugarcane: Contribution of Process-Based Models for
833 Understanding and Mitigating Impacts of Climate Variability and Change on
834 Production, in: Ahmed, M. (Ed.), *Systems Modeling*. Springer Singapore, Singapore,
835 pp. 217–260. https://doi.org/10.1007/978-981-15-4728-7_8

836 Dias, H.B., Inman-Bamber, G., Bermejo, R., Sentelhas, P.C., Christodoulou, D., 2019. New
837 APSIM-Sugar features and parameters required to account for high sugarcane yields in
838 tropical environments. *Field Crops Res.* 235, 38–53.
839 <https://doi.org/10.1016/j.fcr.2019.02.002>

840 Dias, H.B., Inman-Bamber, G., Everingham, Y., Sentelhas, P.C., Bermejo, R., Christodoulou,
841 D., 2020. Traits for canopy development and light interception by twenty-seven
842 Brazilian sugarcane varieties. *Field Crops Res.* 249, 107716.
843 <https://doi.org/10.1016/j.fcr.2020.107716>

844 Dias, H.B., Inman-Bamber, G., Sentelhas, P.C., Everingham, Y., Bermejo, R., Christodoulou,
845 D., 2021a. High-yielding sugarcane in tropical Brazil – Integrating field
846 experimentation and modelling approach for assessing variety performances. *Field*
847 *Crops Res.* 274, 108323. <https://doi.org/10.1016/j.fcr.2021.108323>

848 Dias, H.B., Sentelhas, P.C., 2017. Evaluation of three sugarcane simulation models and their
849 ensemble for yield estimation in commercially managed fields. *Field Crops Res.* 213,
850 174–185. <https://doi.org/10.1016/j.fcr.2017.07.022>

851 Dias, H.B., Sentelhas, P.C., Inman-Bamber, G., Everingham, Y., 2021b. Sugarcane yield future
852 scenarios in Brazil as projected by the APSIM-Sugar model. *Ind. Crops Prod.* 171,
853 113918. <https://doi.org/10.1016/j.indcrop.2021.113918>

854 Donaldson, R.A., 2009. Season effects on the potential biomass and sucrose accumulation of
855 some commercial cultivars of sugarcane. (PhD Thesis). University of KwaZulu-Natal,
856 Faculty of Science and Agriculture, Pietermaritzburg, South Africa.

857 Donaldson, R.A., Redshaw, K.A., Rhodes, R., van Antwerpen, R., 2008. Season Effects on
858 Productivity of Some Commercial South African Sugarcane Cultivars, I: Biomass and
859 Radiation Use Efficiency, in: *Proceedings of the 81st Annual Congress of the South*

860 African Sugar Technologists' Association. Presented at the 81st Annual Congress of the
861 South African Sugar Technologists' Association, Durban, South Africa, pp. 517–527.

862 Du, Y. -C., Nose, A., Wasano, K., 1999. Effects of chilling temperature on photosynthetic rates,
863 photosynthetic enzyme activities and metabolite levels in leaves of three sugarcane
864 species. *Plant Cell Environ.* 22, 317–324. <https://doi.org/10.1046/j.1365-3040.1999.00415.x>

866 Elzhov, T.V., Mullen, K.M., Spiess, A.-N., Bolker, B., Mullen, M.K.M., Suggests, M., 2016.
867 Package 'minpack. lm.' Title R Interface Levenberg-Marquardt Nonlinear Least-Sq
868 Algorithm Found MINPACK Plus Support Bounds.

869 Feng, X., Porporato, A., Rodriguez-Iturbe, I., 2013. Changes in rainfall seasonality in the
870 tropics. *Nat. Clim. Change* 3, 811–815. <https://doi.org/10.1038/nclimate1907>

871 Fox, J., Weisberg, S., Price, B., Adler, D., Bates, D., Baud-Bovy, G., Bolker, B., Ellison, S.,
872 Firth, D., Friendly, M., Gorjanc, G., Graves, S., Heiberger, R., Krivitsky, P., Laboissiere,
873 R., Maechler, M., Monette, G., Murdoch, D., Nilsson, H., Ogle, D., Ripley, B., Short,
874 T., Venables, W., Walker, S., Winsemius, D., Zeileis, A., R-Core, 2023. *car: Companion*
875 *to Applied Regression*.

876 Goldemberg, J., Mello, F.F.C., Cerri, C.E.P., Davies, C.A., Cerri, C.C., 2014. Meeting the global
877 demand for biofuels in 2021 through sustainable land use change policy. *Energy Policy*
878 69, 14–18. <https://doi.org/10.1016/j.enpol.2014.02.008>

879 Hammer, G., Messina, C., Wu, A., Cooper, M., 2019. Biological reality and parsimony in crop
880 models—why we need both in crop improvement! *Silico Plants* 1, diz010.
881 <https://doi.org/10.1093/insilicoplants/diz010>

882 Inman-Bamber, N.G., Jackson, P.A., Hewitt, M., 2011. Sucrose accumulation in sugarcane
883 stalks does not limit photosynthesis and biomass production. *Crop Pasture Sci.* 62, 848–
884 858. <https://doi.org/10.1071/CP11128>

885 Inman-Bamber, N.G., Lakshmanan, P., Park, S., 2012. Sugarcane for water-limited
886 environments: Theoretical assessment of suitable traits. *Field Crops Res.* 134, 95–104.
887 <https://doi.org/10.1016/j.fcr.2012.05.004>

888 Inman-Bamber, N.G., Smith, D.M., 2005. Water relations in sugarcane and response to water
889 deficits. *Field Crops Res.* 92, 185–202. <https://doi.org/10.1016/j.fcr.2005.01.023>

890 IPCC, 2023. Summary for Policymakers. In: *Climate Change 2023: Synthesis Report.*
891 *Contribution of Working Groups I, II and III to the Sixth Assessment Report of the*
892 *Intergovernmental Panel on Climate Change.* IPCC, Geneva, Switzerland.

893 Johnson, I.R., Thornley, J.H.M., Frantz, J.M., Bugbee, B., 2010. A model of canopy
894 photosynthesis incorporating protein distribution through the canopy and its acclimation
895 to light, temperature and CO₂. *Ann. Bot.* 106, 735–749.
896 <https://doi.org/10.1093/aob/mcq183>

897 Jones, M.R., Singels, A., 2018. Refining the Canegro model for improved simulation of climate
898 change impacts on sugarcane. *Eur. J. Agron.* 100, 76–86.
899 <https://doi.org/10.1016/j.eja.2017.12.009>

900 Jones, M.R., Singels, A., Chinorumba, S., Patton, A., Poser, C., Singh, M., Martiné, J.F.,
901 Christina, M., Shine, J., Annandale, J., Hammer, G., 2019. Exploring process-level
902 genotypic and environmental effects on sugarcane yield using an international
903 experimental dataset. *Field Crops Res.* 244, 107622.
904 <https://doi.org/10.1016/j.fcr.2019.107622>

905 Jones, M.R., Singels, A., Chinorumba, S., Poser, C., Christina, M., Shine, J., Annandale, J.,
906 Hammer, G.L., 2021. Evaluating process-based sugarcane models for simulating

907 genotypic and environmental effects observed in an international dataset. *Field Crops*
908 *Res.* 260, 107983. <https://doi.org/10.1016/j.fcr.2020.107983>

909 Jongrunklang, N., Maneerattanarungroj, P., Jogloy, S., Songsri, P., Jaisil, P., 2018.
910 Understanding lodging resistant traits from diverse sugarcane lines. *Philipp. J. Crop Sci.*
911 43, 71–80.

912 Keating, B.A., Robertson, M.J., Muchow, R.C., Huth, N.I., 1999. Modelling sugarcane
913 production systems I. Development and performance of the sugarcane module. *Field*
914 *Crops Res.* 61, 253–271. [https://doi.org/10.1016/S0378-4290\(98\)00167-1](https://doi.org/10.1016/S0378-4290(98)00167-1)

915 Kebalo, F.L., Versini, A., Soulie, J.-C., Ramos, M., Chevalier, L., Chaput, M., Christina, M., in
916 press. Modeling perennial sugarcane growth with the STICS soil-crop model in
917 contrasted environments: calibration and domain of validity. *Field Crops Res.*

918 Kohila, S., Gomathi, R., 2018. Adaptive physiological and biochemical response of sugarcane
919 genotypes to high-temperature stress. *Indian J. Plant Physiol.* 23, 245–260.
920 <https://doi.org/10.1007/s40502-018-0363-y>

921 Leal, M.R.L.V., Horta Nogueira, L.A., Cortez, L.A.B., 2013. Land demand for ethanol
922 production. *Appl. Energy* 102, 266–271.
923 <https://doi.org/10.1016/j.apenergy.2012.09.037>

924 Lenth, R.V., Bolker, B., Buerkner, P., Giné-Vázquez, I., Herve, M., Jung, M., Love, J., Miguez,
925 F., Riebl, H., Singmann, H., 2023. emmeans: Estimated Marginal Means, aka Least-
926 Squares Means.

927 Leroux, M.D., Bonnardot, F., Kotomangazafy, S., Veerabadren, P., Oikil Ridhoine, A., Somot,
928 S., Alias, A., Chauvin, F., 2021. Regional climate projections and associated climate
929 services in the southwest Indian ocean basin EGU21-7029.
930 <https://doi.org/10.5194/egusphere-egu21-7029>

931 Linnenluecke, M.K., Nucifora, N., Thompson, N., 2018. Implications of climate change for the
932 sugarcane industry. *Wiley Interdiscip. Rev.-Clim. Change* 9, e498.
933 <https://doi.org/10.1002/wcc.498>

934 Liu, Y.Y., Li, J., Liu, S.C., Yu, Q., Tong, X.J., Zhu, T.T., Gao, X.X., Yu, L.X., 2020. Sugarcane
935 leaf photosynthetic light responses and their difference between varieties under high
936 temperature stress. *Photosynthetica*. <https://doi.org/10.32615/ps.2020.038>

937 Lloyd, J., Taylor, J.A., 1994. On the Temperature Dependence of Soil Respiration. *Funct. Ecol.*
938 8, 315–323. <https://doi.org/10.2307/2389824>

939 Long, S.P., 1999. 7 - Environmental Responses, in: Sage, R.F., Monson, R.K. (Eds.), *C4 Plant*
940 *Biology, Physiological Ecology*. Academic Press, San Diego, pp. 215–249.
941 <https://doi.org/10.1016/B978-012614440-6/50008-2>

942 Luo, J., Pan, Y.-B., Xu, L., Zhang, Y., Zhang, H., Chen, R., Que, Y., 2014. Photosynthetic and
943 Canopy Characteristics of Different Varieties at the Early Elongation Stage and Their
944 Relationships with the Cane Yield in Sugarcane. *Sci. World J.* 2014, 707095.
945 <https://doi.org/10.1155/2014/707095>

946 Luo, J., Que, Y., Zhang, H., Xu, L., 2013. Seasonal Variation of the Canopy Structure
947 Parameters and Its Correlation with Yield-Related Traits in Sugarcane. *Sci. World J.*
948 2013, 801486. <https://doi.org/10.1155/2013/801486>

949 Magalhães Filho, J.R., 2014. Eficiências associadas à produtividade de cana-de-açúcar e à
950 arquitetura do dossel (PhD Thesis). Instituto Agronômico de Campinas, Campinas,
951 Brasil.

952 Maiorano, A., Martre, P., Asseng, S., Ewert, F., Müller, C., Rötter, R.P., Ruane, A.C., Semenov,
953 M.A., Wallach, D., Wang, E., Alderman, P.D., Kassie, B.T., Biernath, C., Basso, B.,

954 Cammarano, D., Challinor, A.J., Doltra, J., Dumont, B., Rezaei, E.E., Gayler, S.,
955 Kersebaum, K.C., Kimball, B.A., Koehler, A.-K., Liu, B., O’Leary, G.J., Olesen, J.E.,
956 Ottman, M.J., Priesack, E., Reynolds, M., Stratonovitch, P., Streck, T., Thorburn, P.J.,
957 Waha, K., Wall, G.W., White, J.W., Zhao, Z., Zhu, Y., 2017. Crop model improvement
958 reduces the uncertainty of the response to temperature of multi-model ensembles. *Field*
959 *Crops Res.*, Modeling crops from genotype to phenotype in a changing climate 202, 5–
960 20. <https://doi.org/10.1016/j.fcr.2016.05.001>

961 Marin, F.R., Jones, J.W., Royce, F., Suguitani, C., Donzeli, J.L., Filho, W.J.P., Nassif, D.S.P.,
962 2011. Parameterization and Evaluation of Predictions of DSSAT/CANEGRO for
963 Brazilian Sugarcane. *Agron. J.* 103, 304–315. <https://doi.org/10.2134/agronj2010.0302>

964 Marin, F.R., Jones, J.W., Singels, A., Royce, F., Assad, E.D., Pellegrino, G.Q., Justino, F., 2013.
965 Climate change impacts on sugarcane attainable yield in southern Brazil. *Clim. Change*
966 117, 227–239. <https://doi.org/10.1007/s10584-012-0561-y>

967 Marin, F.R., Ribeiro, R.V., Marchiori, P.E.R., 2014. How can crop modeling and plant
968 physiology help to understand the plant responses to climate change? A case study with
969 sugarcane. *Theor. Exp. Plant Physiol.* 26, 49–63. <https://doi.org/10.1007/s40626-014-0006-2>

971 Marin, F.R., Thorburn, P.J., Nassif, D.S.P., Costa, L.G., 2015. Sugarcane model
972 intercomparison: Structural differences and uncertainties under current and potential
973 future climates. *Environ. Model. Softw.* 72, 372–386.
974 <https://doi.org/10.1016/j.envsoft.2015.02.019>

975 Martins, T.D.S., Magalhães Filho, J.R., Cruz, L.P., Machado, D.F.S.P., Erismann, N.M.,
976 Gondim-Tomaz, R.M.A., Marchiori, P.E.R., Silva, A.L.B.O., Machado, E.C., Ribeiro,
977 R.V., 2024. Physiological and biochemical processes underlying the differential sucrose
978 yield and biomass production in sugarcane varieties. *Exp. Agric.* 60, e13.
979 <https://doi.org/10.1017/S0014479724000061>

980 Martins, T.S., Magalhães Filho, J.R., Cruz, L.P., Almeida, R.L., Marchiori, P.E.R., Silva,
981 A.L.B.O., Pires, R.C.M., Landell, M.G.A., Xavier, M.A., Machado, E.C., Ribeiro, R.V.,
982 2025. Light interception and conversion efficiencies and biomass partitioning in
983 sugarcane varieties with varying canopy architecture under subtropical conditions. *Field*
984 *Crops Res.* 322, 109724. <https://doi.org/10.1016/j.fcr.2024.109724>

985 McCormick, A.J., Cramer, M.D., Watt, D.A., 2008. Changes in Photosynthetic Rates and Gene
986 Expression of Leaves during a Source–Sink Perturbation in Sugarcane. *Ann. Bot.* 101,
987 89–102. <https://doi.org/10.1093/aob/mcm258>

988 McCormick, A.J., Cramer, M.D., Watt, D.A., 2006. Sink strength regulates photosynthesis in
989 sugarcane. *New Phytol.* 171, 759–770. <https://doi.org/10.1111/j.1469-8137.2006.01785.x>

991 McCormick, A.J., Watt, D.A., Cramer, M.D., 2009. Supply and demand: sink regulation of
992 sugar accumulation in sugarcane. *J. Exp. Bot.* 60, 357–364.
993 <https://doi.org/10.1093/jxb/ern310>

994 Monteith, J.L., Moss, C.J., Cooke, G.W., Pirie, N.W., Bell, G.D.H., 1997. Climate and the
995 efficiency of crop production in Britain. *Philos. Trans. R. Soc. Lond. B Biol. Sci.* 281,
996 277–294. <https://doi.org/10.1098/rstb.1977.0140>

997 Moore, P.H., Botha, F.C. (Eds.), 2013. *Sugarcane: Physiology, Biochemistry, and Functional*
998 *Biology*, 1st ed. John Wiley & Sons Ltd. <https://doi.org/10.1002/9781118771280>

999 Moore, P.H., Paterson, A.H., Tew, T., 2013. Sugarcane: The Crop, the Plant, and Domestication,
1000 in: *Sugarcane: Physiology, Biochemistry, and Functional Biology*. John Wiley & Sons,
1001 Ltd, pp. 1–17. <https://doi.org/10.1002/9781118771280.ch1>

- 1002 Muchow, R.C., Evensen, C.I., Osgood, R.V., Robertson, M.J., 1997. Yield Accumulation in
1003 Irrigated Sugarcane: II. Utilization of Intercepted Radiation. *Agron. J.* 89, 646–652.
1004 <https://doi.org/10.2134/agronj1997.00021962008900040017x>
- 1005 Muchow, R.C., Spillman, M.F., Wood, A.W., Thomas, M.R., 1994. Radiation interception and
1006 biomass accumulation in a sugarcane crop grown under irrigated tropical conditions.
1007 *Aust. J. Agric. Res.* 45, 37–49. <https://doi.org/10.1071/AR9940037>
- 1008 Olivier, F.C., Singels, A., Eksteen, A.B., 2016. Water and radiation use efficiency of sugarcane
1009 for bioethanol production in South Africa, benchmarked against other selected crops.
1010 *South Afr. J. Plant Soil* 33, 1–11. <https://doi.org/10.1080/02571862.2015.1075231>
- 1011 Parent, B., Tardieu, F., 2012. Temperature responses of developmental processes have not been
1012 affected by breeding in different ecological areas for 17 crop species. *New Phytol.* 194,
1013 760–774. <https://doi.org/10.1111/j.1469-8137.2012.04086.x>
- 1014 Park, S.E., Robertson, M., Inman-Bamber, N.G., 2005. Decline in the growth of a sugarcane
1015 crop with age under high input conditions. *Field Crops Res., Sugarcane*
1016 *physiology: Integrating from cell to crop to advance sugarcane production* 92, 305–320.
1017 <https://doi.org/10.1016/j.fcr.2005.01.025>
- 1018 Peixoto, M. de M., Sage, R.F., 2017. Comparative photosynthetic responses in upland and
1019 lowland sugarcane cultivars grown in cool and warm conditions. *Braz. J. Bot.* 40, 829–
1020 839. <https://doi.org/10.1007/s40415-017-0394-z>
- 1021 Pinheiro, J., Bates, D., DebRoy, S., Sarkar, D., Heisterkamp, S., Van Willigen, B., Ranke, J., R
1022 Core Team, 2022. *nlme: Linear and Nonlinear Mixed Effects Models.*
- 1023 Ribeiro, R.V., Machado, E.C., Magalhães Filho, J.R., Lobo, A.K.M., Martins, M.O., Silveira,
1024 J.A.G., Yin, X., Struik, P.C., 2017. Increased sink strength offsets the inhibitory effect
1025 of sucrose on sugarcane photosynthesis. *J. Plant Physiol.* 208, 61–69.
1026 <https://doi.org/10.1016/j.jplph.2016.11.005>
- 1027 Robertson, M.J., Wood, A.W., Muchow, R.C., 1996. Growth of sugarcane under high input
1028 conditions in tropical Australia. I. Radiation use, biomass accumulation and
1029 partitioning. *Field Crops Res.* 48, 11–25. [https://doi.org/10.1016/0378-4290\(96\)00041-X](https://doi.org/10.1016/0378-4290(96)00041-X)
- 1031 Robinson, N., Fletcher, A., Whan, A., Critchley, C., Wirén, N. von, Lakshmanan, P., Schmidt,
1032 S., 2007. Sugarcane genotypes differ in internal nitrogen use efficiency. *Funct. Plant*
1033 *Biol.* 34, 1122–1129. <https://doi.org/10.1071/FP07183>
- 1034 Saez, J.V., Mariotti, J.A., Vega, C.R.C., 2019. Source-sink relationships during early crop
1035 development influence earliness of sugar accumulation in sugarcane (*Saccharum* spp.).
1036 *J. Exp. Bot.* 70, 5157–5171. <https://doi.org/10.1093/jxb/erz251>
- 1037 Sage, R.F., Peixoto, M.M., Sage, T.L., 2013. Photosynthesis in Sugarcane, in: Moore, P.H.,
1038 Botha, F.C. (Eds.), *Sugarcane: Physiology, Biochemistry, and Functional Biology.* John
1039 Wiley & Sons, Inc., Chichester, UK, pp. 121–154.
1040 <https://doi.org/10.1002/9781118771280.ch6>
- 1041 Santos, C.M.A., Ribeiro, R.V., Magalhães Filho, J.R., Machado, D.F.S.P., Machado, E.C., 2011.
1042 Low substrate temperature imposes higher limitation to photosynthesis of orange plants
1043 as compared to atmospheric chilling. *Photosynthetica* 49, 546–554.
1044 <https://doi.org/10.1007/s11099-011-0071-6>
- 1045 Schwerz, F., Medeiros, S.L.P., Elli, E.F., Eloy, E., Sgarbossa, J., Caron, B.O., 2018. Plant
1046 growth, radiation use efficiency and yield of sugarcane cultivated in agroforestry
1047 systems: An alternative for threatened ecosystems. *An. Acad. Bras. Ciênc.* 90, 3265–
1048 3283. <https://doi.org/10.1590/0001-3765201820160806>

- 1049 Silva, T.G.F. da, 2009. Análise de crescimento, interação biosfera-atmosfera e eficiência do uso
1050 de água da cana-de-açúcar irrigada no submédio do Vale do São Francisco (PhD Thesis).
1051 Universidade Federal de Viçosa, Viçosa, Brasil.
- 1052 Sinclair, T.R., Muchow, R.C., 1999. Radiation Use Efficiency, in: Sparks, D.L. (Ed.), Advances
1053 in Agronomy. Academic Press, pp. 215–265. [https://doi.org/10.1016/S0065-](https://doi.org/10.1016/S0065-2113(08)60914-1)
1054 [2113\(08\)60914-1](https://doi.org/10.1016/S0065-2113(08)60914-1)
- 1055 Sinclair, T.R., Shiraiwa, T., Hammer, G.L., 1992. Variation in Crop Radiation-Use Efficiency
1056 with Increased Diffuse Radiation. *Crop Sci.* 32,
1057 [cropsci1992.0011183X003200050043x](https://doi.org/10.2135/cropsci1992.0011183X003200050043x).
1058 <https://doi.org/10.2135/cropsci1992.0011183X003200050043x>
- 1059 Singels, A., 2013. Crop Models, in: Sugarcane: Physiology, Biochemistry, and Functional
1060 Biology. John Wiley & Sons, Ltd, pp. 541–577.
1061 <https://doi.org/10.1002/9781118771280.ch20>
- 1062 Singels, A., Jackson, P., Inman-Bamber, N.G., 2021. Sugarcane, in: Sadras, V.O., Calderini,
1063 D.F. (Eds.), *Crop Physiology: Case Histories for Major Crops*. Academic Press, pp.
1064 674–713. <https://doi.org/10.1016/B978-0-12-819194-1.00021-9>
- 1065 Singels, A., Jones, M., Marin, F., Ruane, A., Thorburn, P., 2014. Predicting Climate Change
1066 Impacts on Sugarcane Production at Sites in Australia, Brazil and South Africa Using
1067 the Canegro Model. *Sugar Tech* 16, 347–355. [https://doi.org/10.1007/s12355-013-](https://doi.org/10.1007/s12355-013-0274-1)
1068 [0274-1](https://doi.org/10.1007/s12355-013-0274-1)
- 1069 Singels, A., Jones, M.R., Porter, C., Smit, M.A., Kingston, G., Marin, F., Chinorumba, S.,
1070 Jintrawet, A., Suguitani, C., Van Den Berg, M., Saville, G., 2010. The DSSAT4. 5
1071 Canegro model: A useful decision support tool for research and management of
1072 sugarcane production, in: *Proceedings of the International Society of Sugar Cane*
1073 *Technologists*. Presented at the XXVIIth Congress of the International Society of Sugar
1074 Cane Technologists, Veracruz, Mexico.
- 1075 Singels, A., Smit, M.A., 2002. The Effect of Row Spacing on an Irrigated Plant Crop of
1076 Sugarcane Variety NCo376, in: *Proceedings of the South African Sugar Technologists’*
1077 *Association*. pp. 94–105.
- 1078 Singels, A., Smit, M.A., Redshaw, K.A., Donaldson, R.A., 2005. The effect of crop start date,
1079 crop class and cultivar on sugarcane canopy development and radiation interception.
1080 *Field Crops Res.* 92, 249–260. <https://doi.org/10.1016/j.fcr.2005.01.028>
- 1081 Streck, N.A., de Paula, F.L.M., Bisognin, D.A., Heldwein, A.B., Dellai, J., 2007. Simulating
1082 the development of field grown potato (*Solanum tuberosum* L.). *Agric. For. Meteorol.*
1083 142, 1–11. <https://doi.org/10.1016/j.agrformet.2006.09.012>
- 1084 Tejera, N.A., Rodés, R., Ortega, E., Campos, R., Lluch, C., 2007. Comparative analysis of
1085 physiological characteristics and yield components in sugarcane cultivars. *Field Crops*
1086 *Res.* 102, 64–72. <https://doi.org/10.1016/j.fcr.2007.02.002>
- 1087 Thorburn, P.J., Biggs, J.S., Collins, K., Probert, M.E., 2010. Using the APSIM model to
1088 estimate nitrous oxide emissions from diverse Australian sugarcane production systems.
1089 *Agric. Ecosyst. Environ., Estimation of nitrous oxide emission from ecosystems and its*
1090 *mitigation technologies* 136, 343–350. <https://doi.org/10.1016/j.agee.2009.12.014>
- 1091 Thornton, P.K., Ericksen, P.J., Herrero, M., Challinor, A.J., 2014. Climate variability and
1092 vulnerability to climate change: a review. *Glob. Change Biol.* 20, 3313–3328.
1093 <https://doi.org/10.1111/gcb.12581>

- 1094 Van Heerden, P.D.R., Donaldson, R.A., Watt, D.A., Singels, A., 2010. Biomass accumulation
1095 in sugarcane: unravelling the factors underpinning reduced growth phenomena. *J. Exp.*
1096 *Bot.* 61, 2877–2887. <https://doi.org/10.1093/jxb/erq144>
- 1097 Van Heerden, P.D.R., Singels, A., Paraskevopoulos, A., Rossler, R., 2015. Negative effects of
1098 lodging on irrigated sugarcane productivity—An experimental and crop modelling
1099 assessment. *Field Crops Res.* 180, 135–142. <https://doi.org/10.1016/j.fcr.2015.05.019>
- 1100 Venkataramana, S., Gururaja Rao, P.N., Naidu, K.M., 1986. The effects of water stress during
1101 the formative phase on stomatal resistance and leaf water potential and its relationship
1102 with yield in ten sugarcane varieties. *Field Crops Res.* 13, 345–353.
1103 [https://doi.org/10.1016/0378-4290\(86\)90035-3](https://doi.org/10.1016/0378-4290(86)90035-3)
- 1104 Verhulst, P.F., 1838. Notice sur la loi que la population suit dans son accroissement. *Corresp.*
1105 *Math. Phys. Ghent* 10, 113–121.
- 1106 Vianna, M.D.S., Nassif, D.S.P., Dos Santos Carvalho, K., Marin, F.R., 2020. Modelling the
1107 trash blanket effect on sugarcane growth and water use. *Comput. Electron. Agric.* 172,
1108 105361. <https://doi.org/10.1016/j.compag.2020.105361>
- 1109 Vianna, M.S., Williams, K.W., Littleton, E.W., Cabral, O., Cerri, C.E.P., De Jong Van Lier, Q.,
1110 Marthews, T.R., Hayman, G., Zeri, M., Cuadra, S.V., Challinor, A.J., Marin, F.R.,
1111 Galdos, M.V., 2022. Improving the representation of sugarcane crop in the Joint UK
1112 Land Environment Simulator (JULES) model for climate impact assessment. *GCB*
1113 *Bioenergy* 14, 1097–1116. <https://doi.org/10.1111/gcbb.12989>
- 1114 Viaud, P., 2023. Analyse des processus de compétition et de facilitation dans les agrosystèmes
1115 canne-à-sucre x légumineuses. (PhD Thesis). Université de Montpellier, Montpellier,
1116 France.
- 1117 Wang, E., Engel, T., 1998. Simulation of phenological development of wheat crops. *Agric. Syst.*
1118 58, 1–24. [https://doi.org/10.1016/S0308-521X\(98\)00028-6](https://doi.org/10.1016/S0308-521X(98)00028-6)
- 1119 Wang, E., Martre, P., Zhao, Z., Ewert, F., Maiorano, A., Rötter, R.P., Kimball, B.A., Ottman,
1120 M.J., Wall, G.W., White, J.W., Reynolds, M.P., Alderman, P.D., Aggarwal, P.K.,
1121 Anothai, J., Basso, B., Biernath, C., Cammarano, D., Challinor, A.J., De Sanctis, G.,
1122 Doltra, J., Dumont, B., Fereres, E., Garcia-Vila, M., Gayler, S., Hoogenboom, G., Hunt,
1123 L.A., Izaurralde, R.C., Jabloun, M., Jones, C.D., Kersebaum, K.C., Koehler, A.-K., Liu,
1124 L., Müller, C., Naresh Kumar, S., Nendel, C., O’Leary, G., Olesen, J.E., Palosuo, T.,
1125 Priesack, E., Eyshi Rezaei, E., Ripoche, D., Ruane, A.C., Semenov, M.A., Shcherbak,
1126 I., Stöckle, C., Stratonovitch, P., Streck, T., Supit, I., Tao, F., Thorburn, P., Waha, K.,
1127 Wallach, D., Wang, Z., Wolf, J., Zhu, Y., Asseng, S., 2017. The uncertainty of crop yield
1128 projections is reduced by improved temperature response functions. *Nat. Plants* 3,
1129 17102. <https://doi.org/10.1038/nplants.2017.102>
- 1130 Wang, N., Wang, E., Wang, J., Zhang, J., Zheng, B., Huang, Y., Tan, M., 2018. Modelling maize
1131 phenology, biomass growth and yield under contrasting temperature conditions. *Agric.*
1132 *For. Meteorol.* 250–251, 319–329. <https://doi.org/10.1016/j.agrformet.2018.01.005>
- 1133 Wutzler, T., Lucas-Moffat, A., Migliavacca, M., Knauer, J., Sickel, K., Šigut, L., Menzer, O.,
1134 Reichstein, M., 2018. Basic and extensible post-processing of eddy covariance flux data
1135 with REddyProc. *Biogeosciences* 15, 5015–5030. [https://doi.org/10.5194/bg-15-5015-](https://doi.org/10.5194/bg-15-5015-2018)
1136 2018
- 1137 Yin, X., Struik, P.C., Goudriaan, J., 2021. On the needs for combining physiological principles
1138 and mathematics to improve crop models. *Field Crops Res.* 271, 108254.
1139 <https://doi.org/10.1016/j.fcr.2021.108254>
- 1140